ALGERIAN DEMOCRATIC AND POPULAR REPUBLIC
MINISTRY OF HIGHER EDUCATION AND SCIENTIFIC RESEARCH
UNIVERSITY OF MOHAMED BOUDIAF – M'SILA

FACULTY OF SCIENCES
DEPARTMENT OF PHYSICS
N°: Ph/MAT/07/2020

DOMAINE: SCIENCE OF MATTER
FIELD: PHYSICS
OPTION: MATERIAL PHYSICS

Memory Submitted for Obtaining

Diploma of Academic Master

Prepared by: LAZIRI Khadidja

TITLE:

Analytical Study of the Mullite-Cordierite composites prepared by sol-gel method

Defended on: 27/09/2020 before the jury composed of:

OUALI Ameur	**University of Msila**	**president of the jury**
HERAIZ Menad	**University of Msila**	**Supervisor**
SAHNOUNE Foudil	**University of Msila**	**Examiner**
ALLALI Djamel	**University of Msila**	**Examiner**

Academic Year: 2019/2020

Dedication

In the name of **Allah** the most beneficent, the most merciful.

This humble work is dedicated to all beautiful souls that were there through my hardships.

To my moon who raised upon me all the nights with her love, care, sacrifices and her genuinely amazing nature, to my only queen **mom.**

To my sun who raised upon me all the days with protection, love, safe, support and believe in my abilities to fly high with my small wings, to my only king **dad**.

To my stars who overshadowed me with kindness, care and compassion, to my princesses **sisters**.

To my knights who taught me courage and helped me to grow smarter in each step through life, to my light **brothers**.

To part of my joy in life, to my friends **Nadjat**.

Special thanks to **Adala, Latifa**, **Nabila**, **Nissona** and **all my classmates** for the wonderful times

To any person who helped me in any shape or form.

Finally to the one who i treated so badly but she never gave up on me t **myself**.

Acknowledgements

" In the name of ALLAH the most beneficent, the most merciful".

I would like to thank ALLAH for his many blessings and constant mercy upon me through my scientific path and all way long preparing this work.

Secondly I would like to direct my full appreciation and thanks to Prof. **Hraiz Menad** and **Sahnoune Foudil** for their unlimited and constant support and guiding. As well for their noble personality and high scientific ethics in the working space durning accomplishing this work (truly will always be grateful).

I wish also to express my gratitude and thanks to **Hraiz Menad**, **Sahnoune Foudil, OUALI Ameur** and **ALLALI Djamel** for their acceptance to judge this work.

A huge thanks to the physics of materials laboratory and it colleagues and professors for kindly help and encouragement.

Thanks to all my friends at the University of Msila.

Index

Chapter III: RESULTS AND DISCUSSION

General Introduction

General introduction

Being materials older than metals, and materials that had experienced unequaled aesthetic and technical successes before metals, There is increasing interest in the application of advanced ceramic materials in areas as diverse as transport, energy, environment, communications, health, and aerospace.

The increasing scope for the utilization of advanced ceramic materials in a wide range of applications makes the in-depth understanding and studies of processing technologies more necessary than ever before, which can lead to ceramic products and components having the desired performance in service and great properties such as the high resistance of harsh chemical and thermal environments, low electrical coefficient, low toughness.

Mullite ($3Al_2O_3 \cdot 2SiO_2$) and Cordierite ($2MgO \cdot 2Al_2O_3 \cdot 5SiO_2$) each are considered one of the most important ceramics composites in the $MgOAl_2O_3$-SiO_2 system due to it characteristics and properties.

The work presented in this thesis aims at an analysis study for various ratios of the Mullite-Cordierite composites synthesized by Sol-Gel method.

The work is presented as the following:

The first chapter is a bibliographic study which contains five parts:

- ✧ The first part deals with cordierite and it crystal structure, properties and preparation methods.
- ✧ The second part is generalities on mullite such as crystal structure and others like properties, preparation method.
- ✧ The third part talks about mullite- cordierite composites and it properties, preparation methods and application in the industry.
- ✧ The fourth part contain a group of binary and ternary phase diagrams mainly Al_2O_3, SiO_2, MgO ones.
- ✧ The last part is about calculation of activation energy using the non isothermal method.

The second chapter is a review on methods and materials that were used in this work, starting with the used raw materials in preparation method to the deferent types of analysis

that been done, the samples making and ending with the used equipment.

The third chapter is mainly a discussion to the mullite-cordierite composites analysis results which consists of:

- ✧ A thermal study to the behavior of M50C50 using TG/DTG and DSC.
- ✧ A study to the dilatometric results of M50C50.
- ✧ A X-ray diffraction (XRD) and FTIR results study to M50C50.
- ✧ A thermal study on various ratios of mullite-cordierite composites using DSC along with X-ray diffraction (XRD) and it results.
- ✧ The calculation of activation energy E_A and Avrami coefficients m and n in isothermal and non-isothermal treatment for the exothermal peak of Al-Si spinel transformation during heating.

Chapter I
Bibliographic study

I.1 Introduction

A composite material is a material made from two or more constituent materials with significantly different physical or chemical properties that, when combined, produce a material with characteristics different from the individual components. The individual components remain separate and distinct within the finished structure, differentiating composites from mixtures and solid solutions [1, 2].

The new material may be preferred for many reasons. Common examples include materials which are stronger, lighter, or less expensive when compared to traditional materials. More recently, researchers have also begun to actively include sensing, actuation, computation and communication into composites, which are known as Robotic Materials.

I.2 Cordierite

I.2.1 Definition

Cordierite ($2MgO{\cdot}2Al_2O_3{\cdot}5SiO_2$) is an important naturally occurring ceramic material, which occurs in nature as rather rare mineral, it constitutes the phase found in the center of the triaxial diagram of $MgO\text{-}Al_2O_3\text{-}SiO_2$ bounded by the lines joining five eutectic points [3].

I.2.2 Crystal Structure

Cordierite presents a polymorphic structure with three different phases:

- ✧ Cordierite α or indialite a stable hexagonal high temperature form (1450-1460 °C), with lattice parameters a=9.782 A° b=9.782 A° c=9.354 A°
- ✧ The other two forms are much less common and can be prepared only under special conditions:

1. Cordierite β a stable orthorhombic low temperature form (< 1450 °C), and forms hydrothermally below 830°C.
2. A metastable form μ-cordierite, which is a solid solution with β-quartz structure [4-6].

I.2.3 Properties of Cordierite

Cordierite is popular for its low thermal expansion coefficient, low thermal mass, low dielectric loss factor, low density, volume resistivity and high thermal shock resistance, poor corrosion resistance, low toughness [7]. The values of some properties shown in Table (I.1).

Table (I.1): Properties of Cordierite [7].

properties	Value
Density	2.53 g cm^{-3}
thermal conductivity coefficient	3 W m^{-1} K^{-1} (room temp)
Thermal expansion coefficient	1.4~2.6 (x10^{-6}/°C)
Young's modulus E	139~150 GPa.
Modulus of Rupture	117 MPa

I.2.4 Cordierite preparation methods

I.2.4.1 preparation from it basic components

The traditional method for preparing a cordierite powder relies on sintering oxide powders (MgO, Al_2O_3, SiO_2) in proportions equivalent to the chemical composition of cordierite ($2MgO{\cdot}2Al_2O_3{\cdot}5SiO_2$), through raw material reactions in the solid state [8].

Various starting raw materials are used in order to form cordierite phase, generally, alumina as a source of Al_2O_3, talc as a source of MgO and SiO_2, quartz as a source of SiO_2, kaolin or clay as a source of Al_2O_3 and SiO_2 and magnesite as a source of MgO is used [9].

This method is inexpensive, but it's not without some difficulties and flaws, whether in the process of preparation or sintering [8].

I.2.4.2 preparation by Sol-Gel method

It is well known that the sol–gel method has the advantages of excellent control of the chemical composition, and the possibility of reducing the sintering temperature, cordierite produced using alkoxides in recent years, but since the starting materials are expensive and the fabrication processes are complicated [10].

A researcher called Pal and his group prepared cordierite by the sol-gel method using alcoholic oxides and acetate.

A gel powders with the same combination of cordierite ($2MgO.2Al_2O_3.5SiO_2$) were prepared from alcoholic oxide solutions, tetraethyl orthosilicate $Si(C_2H_5O)_4$ (TEOS) $Al(C_4H_9O)_3$ (AlOBt), Magnesium tetrahydrate acetate $Mg(CH_3COO)_2 \cdot 4H_2O$, and the used solvent is $C_3H_8O_2$[8].

I.3 Mullite

I.3.1 Definition

Mullite ($3Al_2O_3 \cdot 2SiO_2$) is a solid solution phase of alumina and silica commonly found in ceramics. Only rarely does mullite occur as a natural mineral, it was originally from the Isle of Mull in Scotland, being the only stable intermediate phase in the Al_2O_3-SiO_2 system at atmospheric pressure, mullite is one of the most important ceramic materials, because of its outstanding electrical, mechanical and thermal properties, and its wide use in traditional and advanced ceramics [11, 12].

I.3.2 Crystal Structure

Mullite ($3Al_2O_3 \cdot 2SiO_2$) crystallizes in the orthorhombic system, space group *Pbam* and lattice parameters a = 0.75499 nm, b = 0.76883 nm, c = 0288379 nm [11, 13].

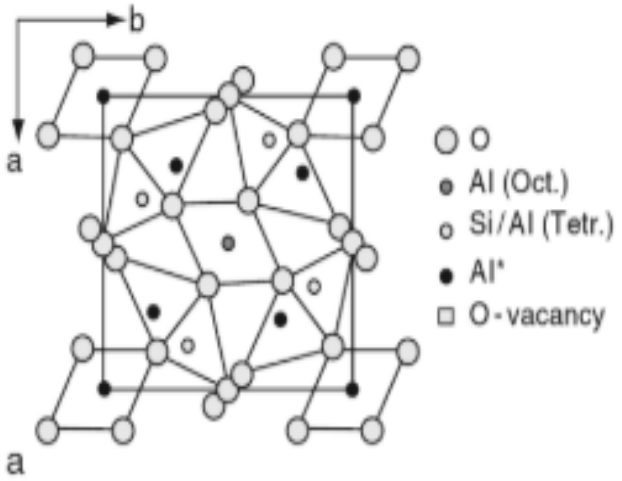

Figure (I.1) Structure of mullite. (a) Average structure [14].

I.3.3 Properties of Mullite

The outstanding properties of mullite are:

Low thermal expansion, low thermal conductivity, and excellent creep resistance. Other favorable characteristics of mullite are suitable high temperature strength and outstanding stability under harsh chemical environments [12]**,** some of it properties are summarized in the table (I.2).

Table (I.2): Properties of Mullite [12, 13].

Properties	Value
Density	3 .1 g cm^{-3}
Thermal conductivity coefficient	6 W m^{-1} K^{-1} (room temp)
Thermal expansion coefficient	4.1(x 10^{-6} $°C^{-1}$) (300-1000°C)
Young's modulus E	250 GPa
Poisson's ratio	0.28
Enthalpies ΔH_f	21 KJ mol^{-1} (room temp)
Entropy $S°_{298\ K}$	269.76 J mol^{-1} K^{-1}
Hardness H_V	~14 GPa
toughness	~2.5 MPa $m^{1/2}$

I.3.4 Chemical properties

Mullite is compound with stoichiometries ranging from relatively silica-rich $3Al_2O_3.2SiO_2$ (3:2 mullite) to alumina-rich $2Al_2O_3.SiO_2$ (2:1 mullite), and it chemical formula is often given by $Al_2(Al_{2+2x}Si_{2-2x})O_{10-x}$, where x = 0 corresponds to sillimanite, x = 0.25 corresponds to 3:2 mullite [11].

I.3.5 Mullite preparation methods

There are many methods to synthesize mullite such as:

I.3.5.1 Mullite preparation from its basic components

Clay and kaolin generally are multiphase minerals, the most frequently used method to obtain pure mullite consists of mixing alumina Al_2O_3 and silica SiO_2 in stoichiometric quantities, and after grinding, pelletizing, it get heated at relatively high temperature (1500-1600°C).

The purity of the mullite obtained depends on that of the raw materials:

$$3Al_2O_3 + 2SiO_2 \rightarrow (3Al_2O_3 \cdot 2SiO_2)$$

This reaction was notably used by Kleebe to study the mechanism of formation and the microstructure of mullite [15].

I.3.5.2 Mullite preparation by adding alumina to kaolinite

Mullite was first identified as the product of heating kaolinitic clays, resulting in a compound with an approximate alumina-to-silica molar ratio of 3:2.

The order of reaction proceeds as follows:

$$Al_2Si_2O_5(OH)_4 \xrightarrow{450°C} 2(Al_2O_3 \cdot 2SiO_2) + 2H_2O$$

Kaolinite Metakaolinite

$$2(Al_2O_3 \cdot 2SiO_2) \xrightarrow{925°C} 2Al_2O_3 \cdot 3SiO_2 + SiO_2$$

Metakaolinite spinel (Al,Si) + amorphous

$$2Al_2O_3 \cdot 3SiO_2 \xrightarrow{1100°C} 2(Al_2O_3 \cdot SiO_2) + SiO_2$$

spinel (Al,Si) Pseudomullite

$$3(Al_2O_3 \cdot SiO_2) \xrightarrow{1400°C} 3Al_2 \cdot 2SiO_2 + SiO_2$$

Pseudomullite Mullite + cristobalite

Excess corundum (Al_2O_3) may be added, and the system get heated at higher temperatures to minimize free SiO_2 [11], due to kaolinite chemical formula (Al_2O_3,2SiO_2, 2H_2O) is deficient in aluminum compared to stoichiometric mullite so it is necessary to add alumina to obtain 3: 2 mullite [15].

I.3.5.3 Mullite preparation by Sol-gel method

A Sol-Gel process involves the formation of a homogeneous solution of raw materials, and

the subsequent gelation of the solution to form a porous amorphous oxide.

Upon firing, densification may proceed to give a glass or a polycrystalline ceramic. Most frequently, organometallic compounds such as alkoxides are dissolved in alcohol to give a homogeneous solution, through direct addition of water, or exposure to the atmosphere. Many factors influence the formation of a gel, among the most important are the amount of water added, the nature and concentration of a catalyst, the solvent, and the sequence of mixing. The freshly formed gel traps solvents and reaction liquids in its pores, which can normally be extracted at temperatures below 100°C, heat treatment and sintering, are required to densify the gel [16].

Recent work on mullite synthesis has focused on variations of sol–gel methods, three categories of gels are usually made:

- Single-phase (type I) mullite precursor gels have near atomic level homogeneous mixing, the precursors transform into an alumina-rich mullite at about 980 °C, These gels are formed from the simultaneous hydrolysis of the aluminum and silicon sources for example, it can be synthesized from tetraethylorthosilicate (TEOS) and aluminum nitrate nonahydrate in ethanol, which had been gelled at 60 °C for several days by a hydrolysis-polymerization reaction.

- Type II diphasic gels comprised two sols with mixing on the nanometer level,These gels after drying consist of boehmite and noncrystalline SiO_2, which at ~350 °C transform to γ-Al_2O_3 and noncrystalline SiO_2.

- Type III diphasic gels contain precursors that are non-crystalline up to 980 °C and then form.

γ-Al_2O_3 and non-crystalline SiO_2 [11].

I.4 MULLITE-CORDIERITE COMPOSITE

I.4.1 Definition

Mullite-Cordierite composites represent an important technological class of materials for use in the electronics packaging industry, previous studies of these composite materials have been primarily concerned with their synthesis, dielectric and mechanical properties.

These materials have a lower dielectric constant than alumina, at present a commonly used

substrate material, this composites expected to achieve a higher performance [17].

I.4.2 Properties

Mullite-Cordierite support each other making this composite useable in so many application due it excellent mechanical properties, energy saving effect, and other properties shown in Table (I.3).

Table (I.3) The properties of Mullite-Cordierite composite [18].

properties	Value
Density	high
Thermal shock resistance	375°C (of 40% cordierite)
Thermal stability	High
Thermal expansion	Low
Thermal conductivity	Low

I.4.3 Mullite-Cordierite preparation methods

Preparations of Mullite-Cordierite powders by different methods have been tried.

- ✧ In one of the processes, cordierite and mullite powders were prepared separately, and mixed to get the required composition, difficulties such as sintering these composites below the melting point of cordierite (1455 °C) were encountered .
- ✧ Another method describes a process for synthesis of cordierite-rich composites using metal alkoxides.
- ✧ Mullite- Cordierite composite powders prepared by the sol-gel method, using inorganic colloidal suspensions, containing up to 60% by weight of cordierite [19].

I.4.4 Applications

As composite Mullite-Cordierite are used as:

- ✧ An ideal material for heavy clay industries.

- ✧ Used in shuttle kilns, tunnel kilns and roller kilns.
- ✧ High temperature filtration applications as ceramic filters.
- ✧ As electrical porcelains.
- ✧ Catalytic converter substrates for exhaust gas control in automobiles.
- ✧ Packing materials in electronic packing [20].

I.5 PHASE DIAGRAMS

I.5.1 The Al_2O_3-SiO_2 System

The Al_2O_3-SiO_2 system contains the compositions of a wide range of alumina-silicate refractories; these include silica, semisilica, fireclay, low alumina, mullite, high alumina, and corundum, phase diagram shown in Figure (I.2). The diagram is characterized by its two end members, Al_2O_3 and SiO_2, and an intermediate compound mullite $3A1_2O_3 \cdot 2SiO_2$, and there are two eutectics in the system:

One between cristobalite and mullite at 1595 °C and the other at 1840 °C between mullite and corundum [21. 22].

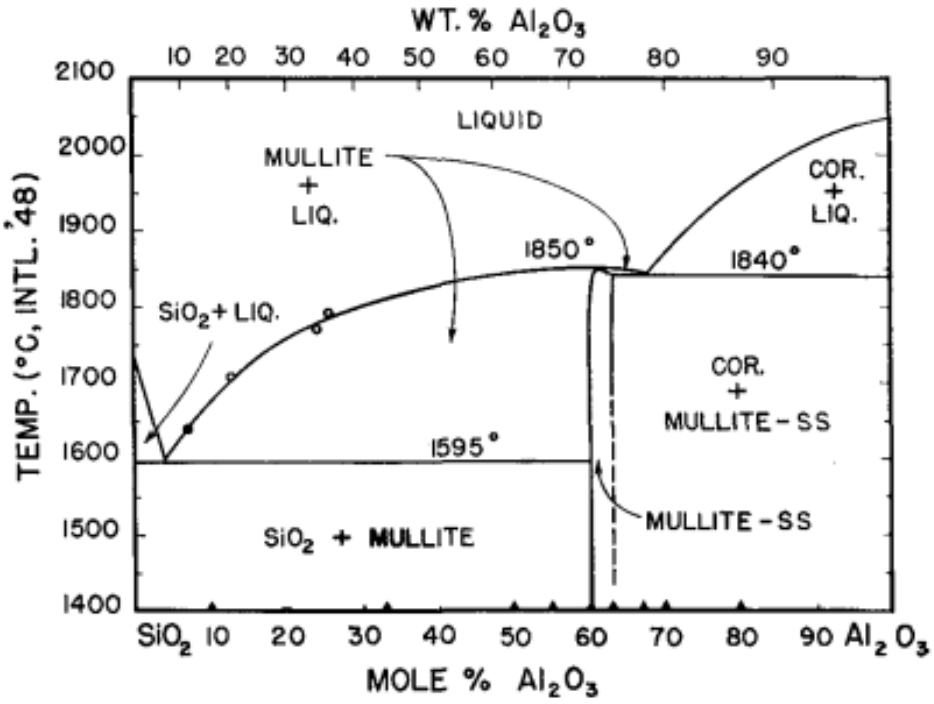

Figure (I.2) The Al_2O_3-SiO_2 phase diagram [22].

I.5.2 The MgO-Al_2O_3 System

The MgO–Al_2O_3 phase diagram is shown in Figure (I.3), it has two eutectic reactions, and an intermediate phase MgO·Al_2O_3. The MgO–Al_2O_3 system is considered as two separate phase diagrams, the components for one being MgO and MgO·Al_2O_3, and for the other being MgO·Al_2O_3 and Al_2O_3, and any small quantity of MgO in Al_2O_3 can decrease it melting point considerably, even though MgO has a high melting point [23].

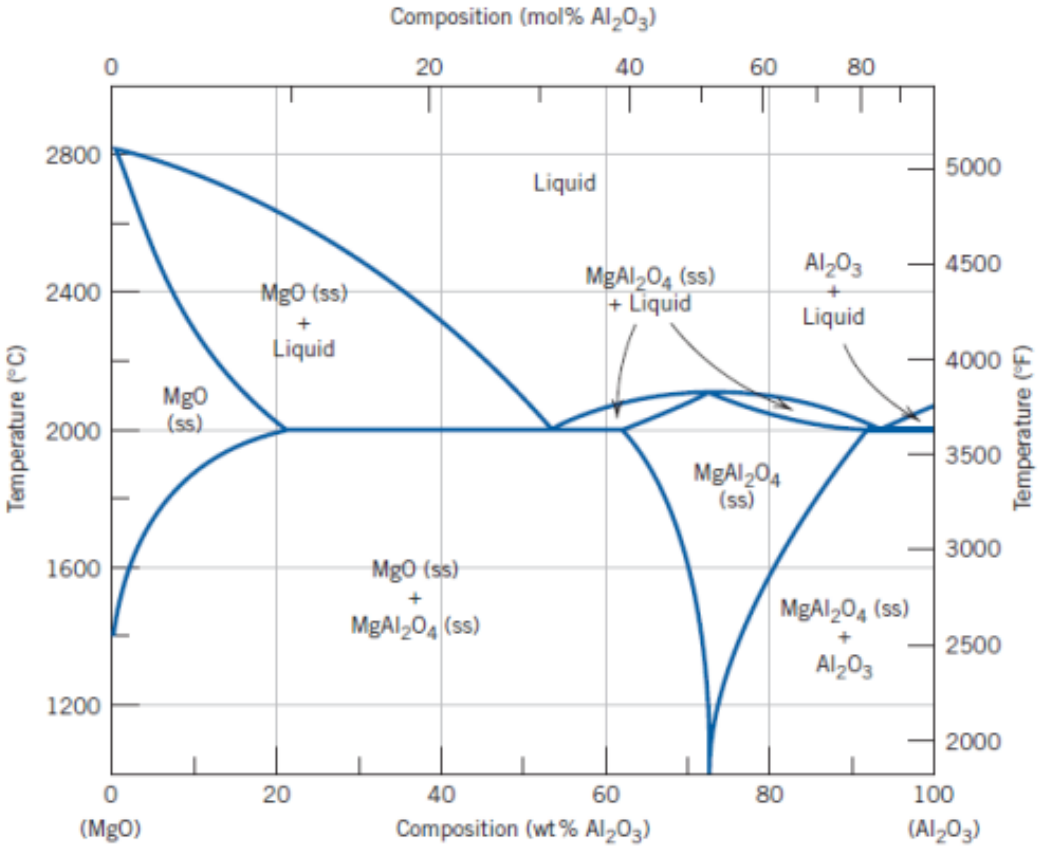

Figure (I.3) The MgO–Al_2O_3 phase diagram [23].

I.5.3 The MgO-SiO_2 system

The MgO-SiO_2 shows the relations between the pyroxenes and the olivines, in the pyroxene enstatite, MgO·SiO_2, melts incongruently with formation of the olivine, forsterite, 2MgO·SiO_2, and more silicious liquid, the phase-equilibrium diagram shown in Figure (I.4) MgO melts at 2800 °C, and forms a eutectic with magnesium orthosilicate (forsterite).

The chemistry of the magnesium metasilicates is complex and was not clearly understood until Schairer (1954) summarized the older work and clarified relations among the various forms.

$MgO \cdot SiO_2$ melts incongruently at 1557 °C to forsterite and more silicious liquid, it becomes completely liquid on the forsterite liquidus curve [24].

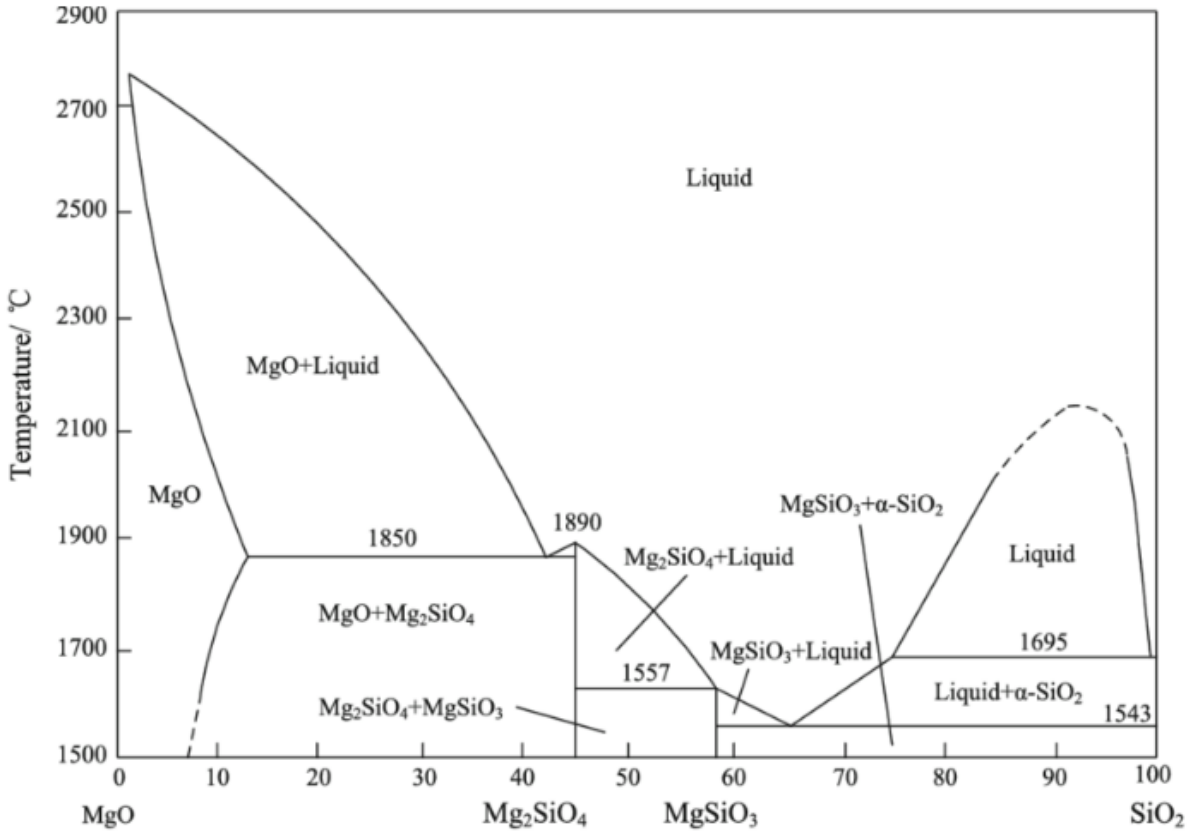

Figure (I.4) The $MgO\text{-}SiO_2$ phase diagram [24].

I.5.3 The $MgO\text{-}Al_2O_3\text{-}SiO_2$ system

The $MgO\text{-}Al_2O_3\text{-}SiO_2$ system is of considerable importance to the ceramic industry, and many of compositions including $Al_2O_3 \cdot SiO_2$, forsterite, mullite, and spinel are used in refractories high temperature furnace linings [25].

A variety of the features are illustrated in Figure (I.5).

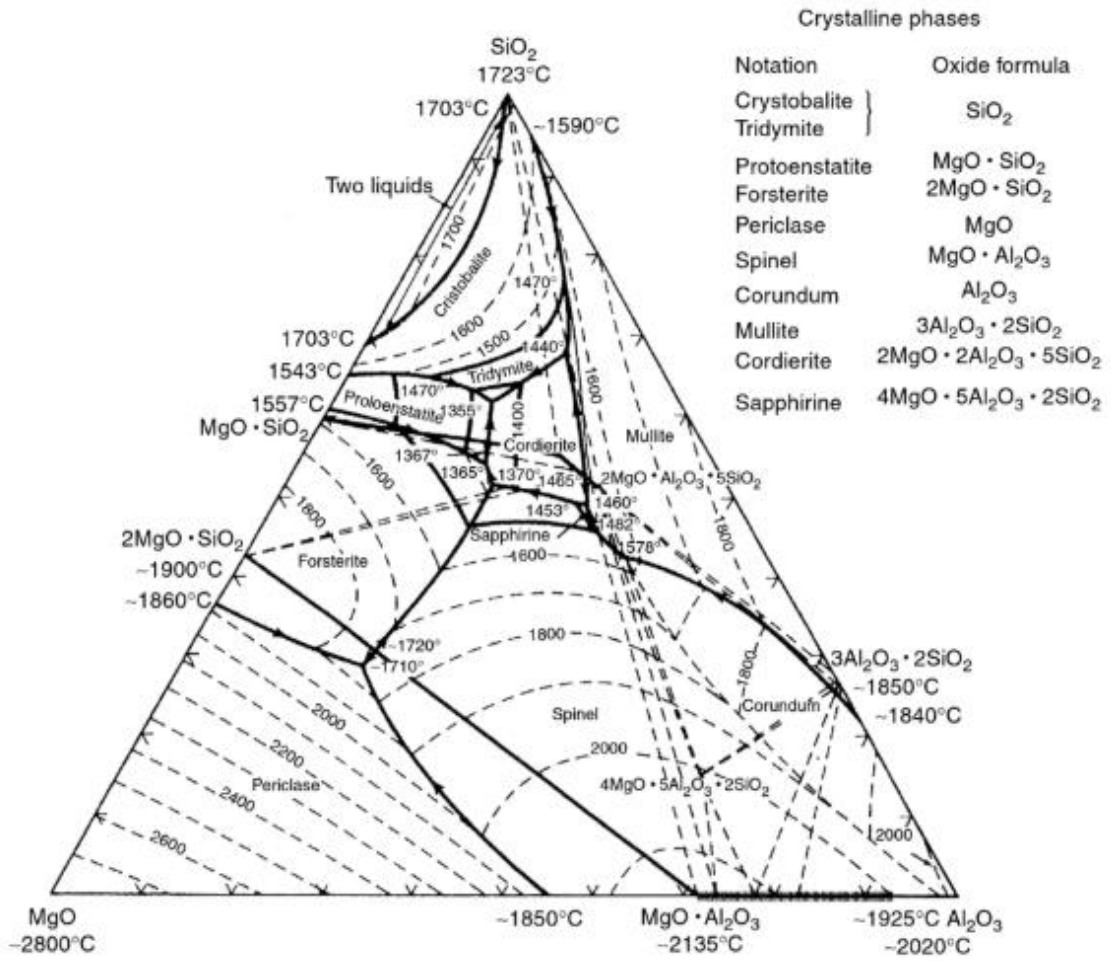

Figure (I.5) The MgO-Al_2O_3-SiO_2 System [25].

I.6 Activation Energy (E_A) Calculation

I.6.1 Non-Isothermal analysis

In a non-isothermal DTA experiment, the temperature change linearly with time at a known heating rate φ (dT/dt), and to calculate the activation energy E_A we will use the following methods:

- ✧ Kissinger method $\ln(\frac{\varphi}{T_P^2}) = -\frac{E_A}{RT_p} + C_1$
- ✧ Boswell method $\ln(\frac{\varphi}{T_P}) = -\frac{E_A}{RT_p} + C_2$
- ✧ Ozawa method $\ln(\varphi) = -1.0518\frac{E_A}{RT_p} + C_3$

$C_{1, 2, 3}$: constant, E_A : activation energy, T_p: maximum of crystallization peak, R: is the ideal gas constant [8].

The value of the Avrami exponent is determined form the shape of the crystallization exothermal peak, and it is related to T_p as:

$$n = \frac{2.5\,\mathrm{RT_P^2}}{\Delta T}\frac{}{E_A}$$

ΔT: the width of crystallization peak at half maximum.

Another kinetic approach commonly used to analyse DTA data is Kissinger method, which is written as:

$$\ln(\frac{\varphi}{T_P^2}) = -\frac{E}{RT_C} + C_4$$

Matusita have proposed a modified form of Kissinger equation as:

$$\ln(\frac{\varphi^n}{T_P^2}) = -\frac{mE}{RT_P} + C_5$$

n: Avrami parameter that indicates the crystallization mode.

m: a numerical factor that depends on the dimensionality of crystal growth [26].

Chapter II
Materials and methods

II.1 The raw materials used

we used in our study some materials, shown in Figure (II.1).

- Aluminum nitrate nanohydrate $Al(NO_3)_3 \cdot 9H_2O$.
- Magnesium nitrate hexahydrate $Mg(NO_3)_2 \cdot 6H_2O$.
- TEOS (formally named tetraethyl orthosilicate) $Si\ (C_2H_5O)_4$.
- Ethanol (C_2H_5OH).

Figure (II.1) the raw materials used.

II.2 Experimental Methods

II.2.1 The preparation of Mullite-Cordierite composite powder

In this study, we prepared various ratios of Mullite-Cordierite composite powders, using Sol-Gel method according to the following process:

a. Measure the mass of $Al(NO_3)_3 \cdot 9H_2O$ and $Mg(NO_3)_2 \cdot 6H_2O$ powder, TEOS and the deionisedwater, ethanol volume according to the chosen ratio of M-C shown in Table **(**II.1) (TEOS to ethanol ratio is 1:4, and water to TEOS ratio is 20:1).
b. Dissolve $Al(NO_3)_3 \cdot 9H_2O$ and $Mg(NO_3)_2 \cdot 6H_2O$ in deionised water.
c. Dissolve TEOS in ethanol.
d. Mix the previous solutions together using magnatic stirrer at 25°C for 2 hours (till obtaining transparent solution).
e. Drying in furnace at 60°C for 48 hours, a gel will form.
f. Dry it in furnace at 120°C for 24 hours.

g. Grind the formed product using mortar and pestle (kept for further use).

- The formed powders of each Mullite-Cordierite composite shown in Figure (II.2).
- The flowchart of the synthesis is presented in Figure (II.3).

Table (II.1) the compounds of each Mullite-Cordierite composite.

M-C	M(NAl) (g)	M(NMg) (g)	M(TEOS) (g)	V H_2O (ml)	V Ethanol (ml)
100:00	13.3496	0	2.4967	53.5208	9.9870
95:05	13.0062	0.1108	2.5992	55.7176	10.3969
90:10	12.6628	0.2216	2.7017	57.9143	10.8068
85:15	12.3195	0.3324	2.8042	60.1110	11.2167
80:20	11.9761	0.4432	2.9067	62.3078	11.6266
50:50	9.9159	1.1079	3.5215	75.4883	14.0861
00:100	6.4822	2.2158	4.5463	97.4557	18.1852

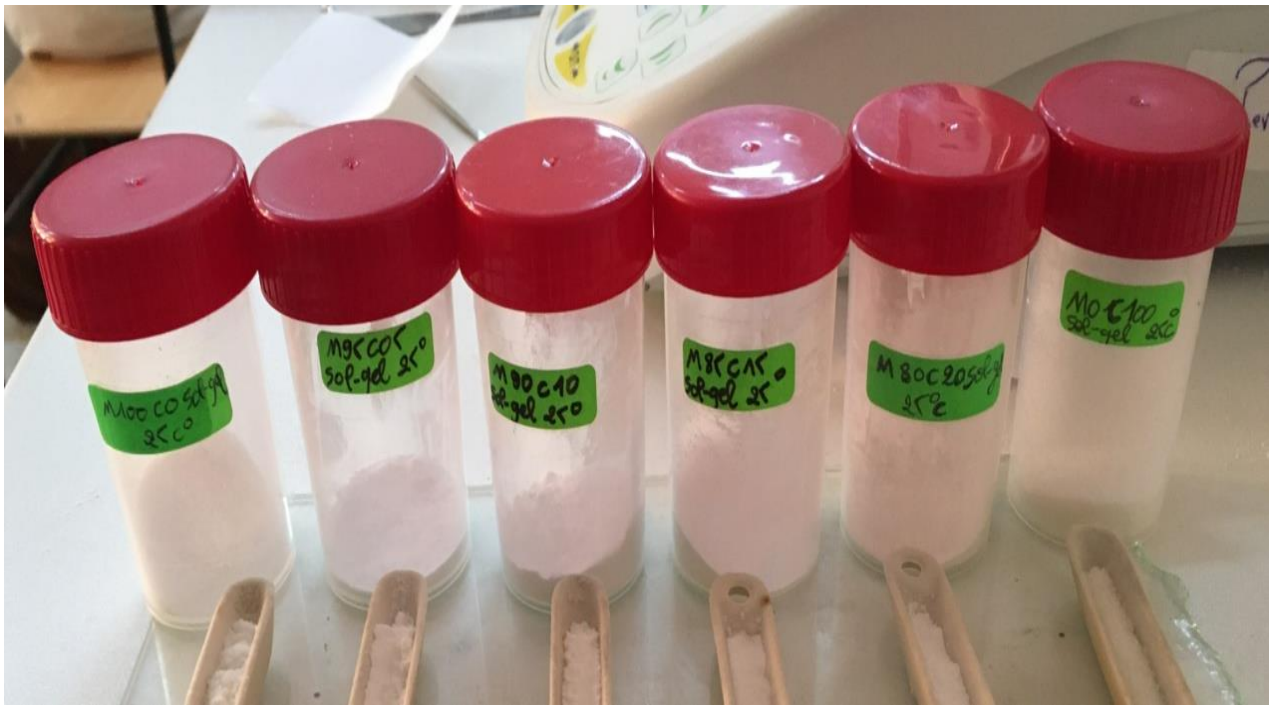

Figure (II.2) samples of Mullite-Cordierite composite.

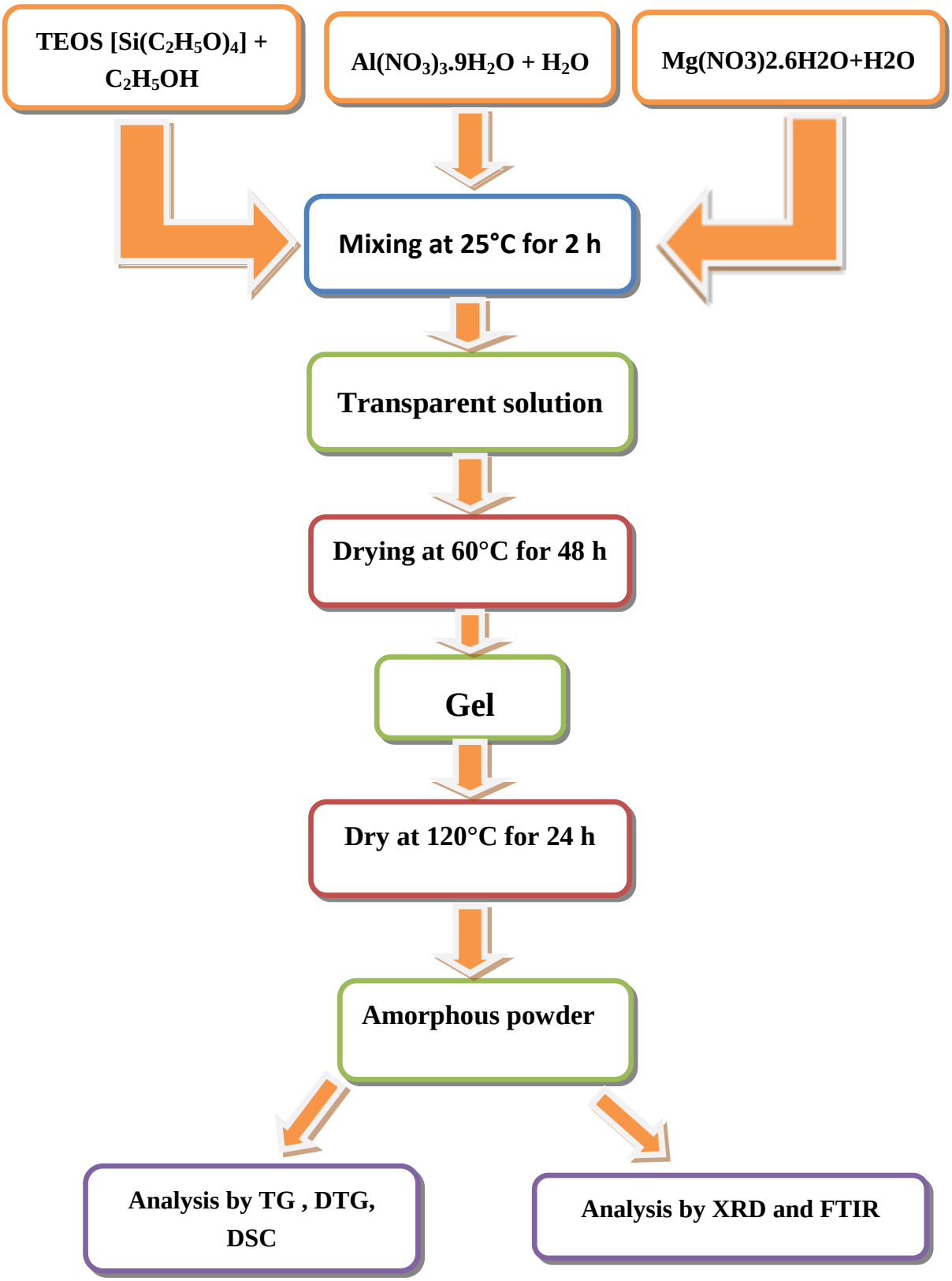

Figure (II.3) Flowchart of the Mullite-Cordierite powder preparation and analyzing.

II.2.2 Differential Scanning Calorimetry DSC, Thermogravimetric & Differential Thermal TGA/DTG Analysis

In order to determine the phase transformations that occur during the heat treatment of each Mullite-Cordierite composite powder, a TG/DTG and DSC experiments were carried out at up to different high temperatures at constant heating rate 30°C min^{-1} for all M-C powders (100:00, 95:05, 90:10, 85:15, 80:20), using LABSYS EVO DTA/DSC-TG SETARAM equipment.

- M-C(50:50) were heated at (910, 1000, 1095, 1185, 1260, 1320, 1420°C) at a constant heating rate of 30°Cmin^{-1}.
- M-C (50:50) was heated at 1430 °C in four constant heating rates 20, 30, 40, 50°Cmin^{-1}.

II.2.3 XRD Analysis

After each previous analysis, the powders are analyzed using a diffractometer MRD, PANalytical (ISM) with Cu(K_α) radiation of a wavelength 0.15418 nm in order to characterize it and the present phases, the 2θ range of XRD patterns were preformed between 05° to 80°.

II.2.4 FTIR Analysis

In order to observe and identify the chemical properties (all chemical compositions and bonds) of previous samples, a FTIR analysis were performed using FTIR-8300 SCSI instrument sending IR radiation of about 4000 to 200 cm^{-1}.

II.2.4.1 Preparation of samples

To prepare FTIR analyzing specimens shown in Figure (II.4), the following procedure were used:

✧ Dry KBr salt at 120°C for 1day.

✧ Add KBr salt to the powder (at mass ratio of specimen to KBr of 1:100).

- ✧ Then grind it well using mortar and pestle for 1~2 min.
- ✧ Use a hydraulic press after cleaning it to shape the sample into a transparent disc (press for 4 min under 80 KN).

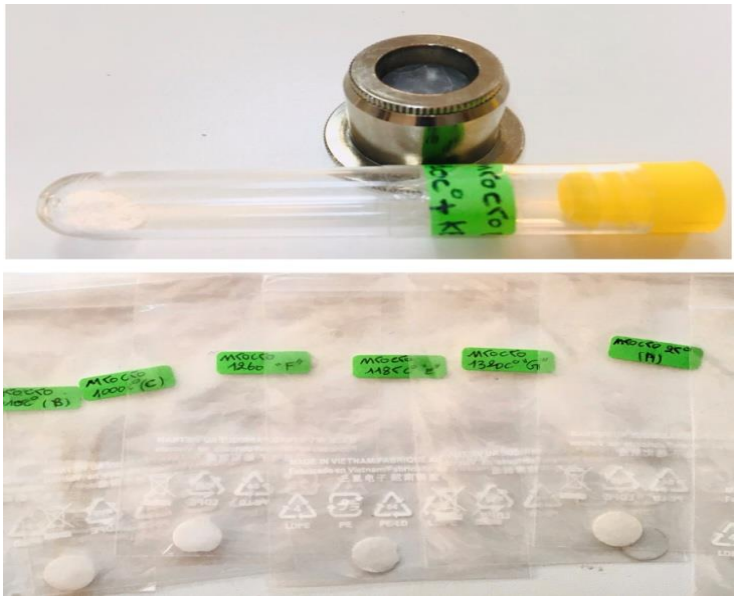

Figure (II.4) FTIR analysis samples.

II.3 The Used Equipment

II.3.1 The FTIR spectroscopy

Infrared spectroscopy is a great technique for materials analysis in laboratories for over seventy years, FTIR equipment shown in Figure (II.5), this technique represents a fingerprint of a sample with absorption peaks which correspond to the frequencies of vibrations between the bonds of atoms making up the material.

The FTIR method uses IR radiation of about 10000 to 100 cm^{-1} that pass through a sample, some of the infrared radiation is absorbed by the sample, some of it pass through (transmitted), the resulting signal at the detector presented as a spectrum, typically from 4000cm^{-1} to 400cm^{-1}, and because each different material is a unique combination of atoms, no two compounds produce the exact same infrared spectrum, therefore we can get an identification (qualitative analysis) of every different kind of material.

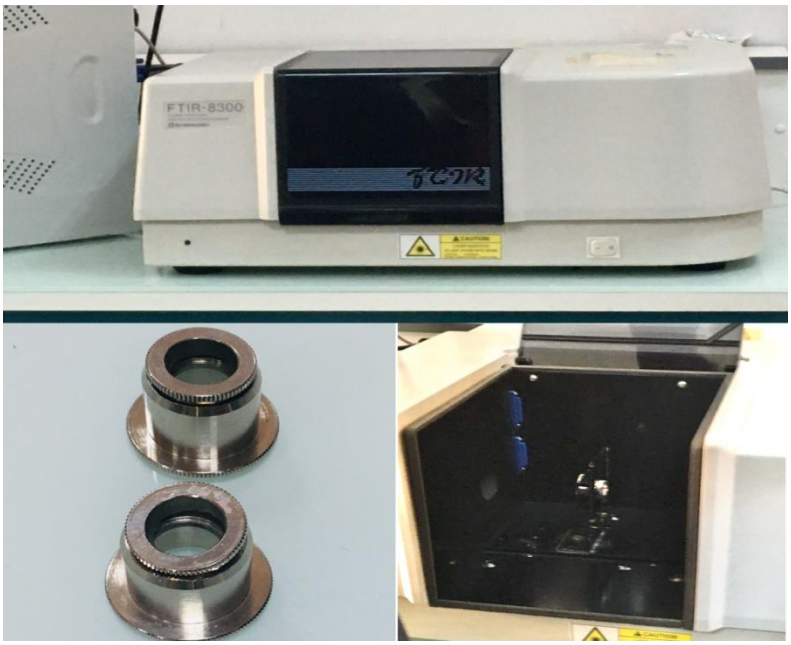

Figure(II.5) a FTIR equipment type FTIR-8300 SCSI.

II.3.2The Diffractometer

A diffractometer shown in Figure (II.6) is an instrument for analyzing the structure of crystalline substance from the scattering pattern produced when a beam of radiation (such as X-rays) strikes it, the angles at which the crystals diffract the beam into the detector corresponds to planes of the crystals, according to Bragg's law:

$$2d_{hkl} \sin\theta = n\lambda$$

n: the order of reflection.

λ: wavelength of the incident wave.

d: the inter-planner distance.

θ: the angle at which X-rays of wavelength are reflected.

Each crystal has a characteristic pattern of diffraction angles and corresponding intensity of the diffracted beam.

Figure(II.6) a diffractometer MRD, PANalytical (ISM)

II.3.3 Thermogravimetric Analysis (TGA), Differential Scanning Calorimet (DSC) and Differential Thermal Analysis DTA

TG: thermogravimetry is a technique measuring the variationin mass of a sample when it under goes temperature scanning in a controlled atmosphere, this variation in mass can be either a loss of mass (vapor emission) or a gain of mass (gas fixation)

DTA: differential thermal analysis is a technique measuring the difference in temperature between a sample and a reference (a thermally inert material) as a function of the time or the temperature, when they undergo temperature scanning in a controlled atmosphere, this method enables any transformation to be detected all the categories of materials.

DSC: differential scanning calorimetry is a technique determining the variation in the heat flow given out or taken in by a sample when it undergoes temperature scanning in a controlled atmosphere, with heating or cooling any transformation taking place in a material is accompanied by exchange of heat, DSC enables the temperature of this transformation to be

determined and the heat from it to be quantified. The equipment used for the previous analyzes is shown in Figure (II.7).

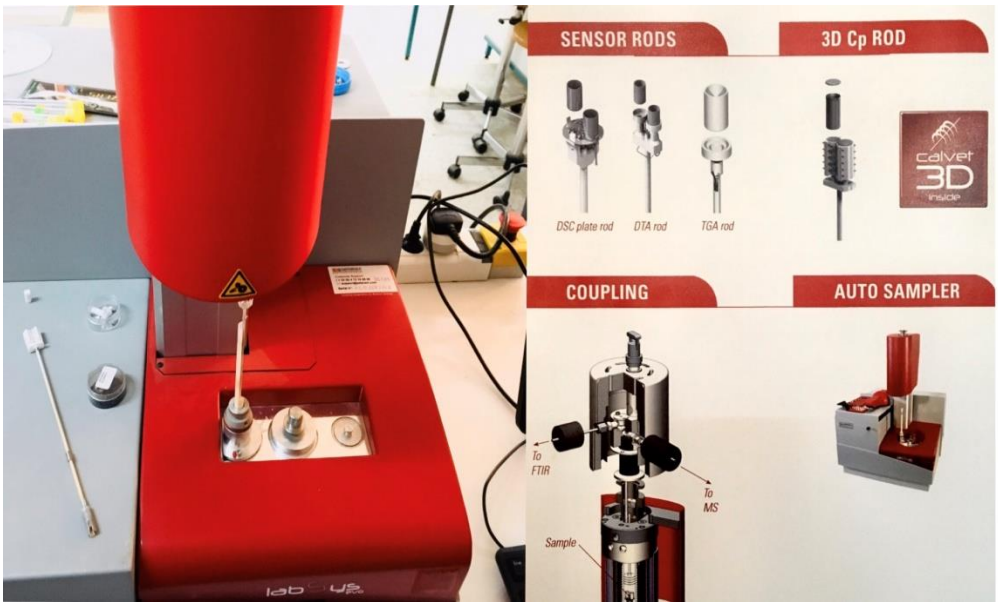

Figure (II.7) a LABSYS EVO DTA/DSC-TG SETARAM equipment.

II.3.4 The Furnace

Most of the heat treatment were done using NABERTHEM furnace, which can reatch 1700°C as it maximum temperture shown in Figure (II.8), along with other two furnce.

Figure (II.8) furnace type Neberthem.

II.3.5 The hydraulic press

A hydraulic press shown in figure (II.9) was used to form FTIR samples, it can ably

120 KN at maximum pressure.

Figure (II.9) hydraulic press.

II.3.6The Electromagnetic balance

An electromagnetic balance type aeADAM Nimbus shown in Figure (II.10) were used to weight the raw materials and samples.

Figure (II.10) Electromagnetic balance type aeADAM Nimbus.

II.3.7 mortar &pestle

A mortar & pestle shown in Figure (II.11) were used to grind KBr and the formed powders.

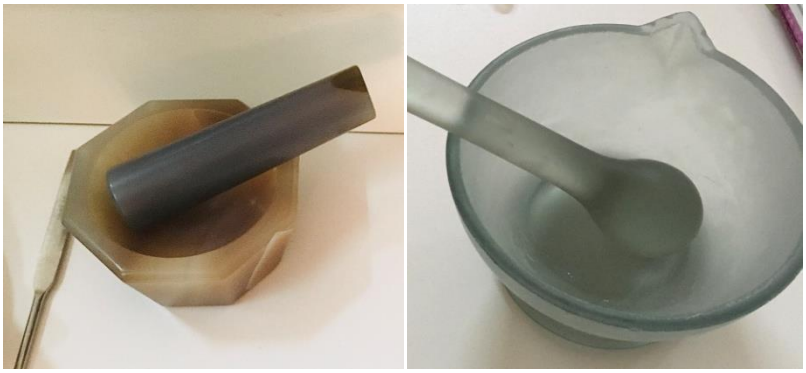

Figure (II.11)mortar &pestle

II.3.8 magnetic stirrer

A magnetic stirrer type AGIMATIC-N shown in Figure (II.12) , was used to mix dissolved raw materials while preparing solutions.

Figure (II.12) magnetic stirrer type AGIMATIC-N.

Chapter III
Results And Discussion

III.1 Introduction

In this chapter we will present the experimental results of Mullite-Cordierite composites obtained by Sol-Gel method, and analyzed by TG/DTG, DSC, DIL, FTIR, and XRD in the following parts:

- Presenting the results and discussion of M50C50 according to the thermal study and XRD, FTIR study.
- Presenting the results and of various MxxCyy ratios according to the DSC and XRD study.
- Presenting calculation results of the activation energy and Avrami parameters to the exothermal peak for Al-Si spinel phase according to the isothermal and non-isothermal method.

III.2 Thermal Study

III.2.1 Dilatometric Study

We took a quantity of M50C50 equivalent powder in order to form a disk sample needed to use on dilatometer according to the experimental conditions.

Figure (III.1) shows linear shrinkage curve a function of T (°C) for mixture M50C50, and its first derivative heated from room temperature to 1400 °C, at heating rate of 11°C/min.

It can be seen from the results the following:

- ✧ A relatively large linear shrinkage about 9.43 % start at 739 °C and end at 1012.4 °C, with maximum shrinkage rate at 893 °C is related to Al-Si spinel phase formation, and this shrinkage is associated with a decrease in this sample volume.
- ✧ From 1066 °C to 1148 °C a linear shrinkage about 0.8 % occurs, with maximum shrinkage rate at 1108 °C which is associated to the formation of mullite phase.
- ✧ A relatively small linear shrinkage about 0.4 % start at 1233 °C and end at 1288 °C, with maximum shrinkage rate at 1260 °C is related to the formation of μ-cordierite phase leading to elongation and increasing in volume.
- ✧ The last linear shrinkage start at 1289 °C and end at 1396 °C, with maximum shrinkage rate at 1331 °C which is associated to the formation of α-cordierite phase,

this transformation cause an increase in volume and elongation about 0.2 %.

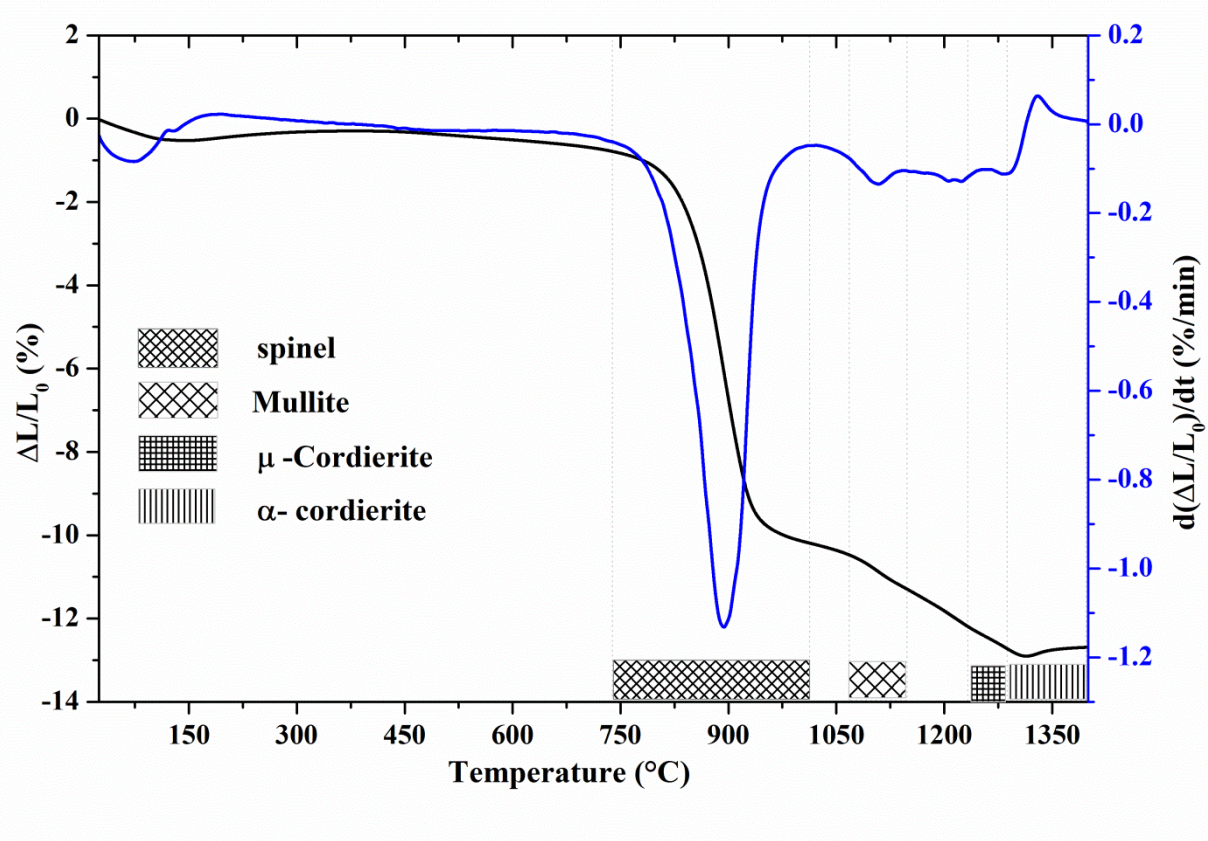

Figure (III.1) Linear shrinkage curve and its first derivative for mixture M50C50 treated at heating rate of 11°C/min.

III.2.2 Thermogravimetric Analysis (TGA) and differential Scanning Calorimetric (DSC) study

The figure (III.2) represent the mass loss and it first derivation (TG/DTG) curves of mixture M50C50 treated from room temperature to 1000 °C, at heating rate of 30 °C/min.

The TG/ DTG curve shows:

- ✧ Only one weight loss occurred between 100 °C to 700 °C and it is probably attributed to the existed three intervals (endothermic peaks).
- ✧ The first interval approximately at 194 °C is probably attributed to the loss of absorbed water.
- ✧ The second interval approximately at 296.2 °C is probably attributed to decomposition of aluminum nitrate.
- ✧ The third interval approximately at 376.6 °C approximately is attributed to the organic decomposition (TEOS decomposition).

✧ The mass loss of the sample is almost 51.2 % during the heating treatment.

Figure (III.3) shows the typical DSC curve of M50C50 treated from room temperature to 1420°C with heating rate 30°C/min, it is indicating the presence of three endothermic peaks, and four exothermic peaks in the temperature range of 700 to 1420 °C, located at 957 °C, 1144 °C,1255 °C, 1365 °C respectively.

✧ The first exothermal peak at temperature 957 °C can be assigned to the formation of Al-Si spinel phase.

✧ The second exothermal peak almost at 1144 °C is associated to the formation of mullite phase.

✧ The third exothermal peak approximately at 1255 °C is properly related to μ-cordierite phase formation.

✧ The last exothermal peak at 1365 °C is related to α-cordierite phase formation [27, 28].

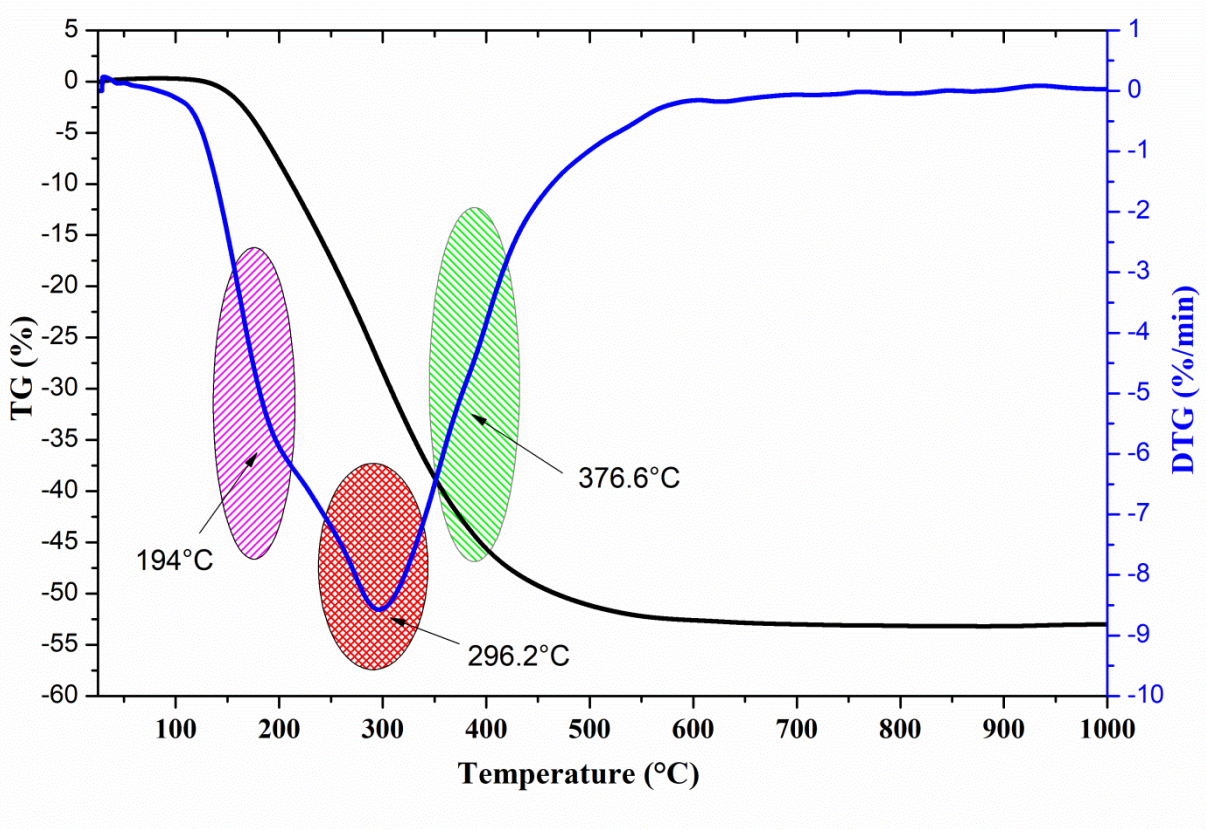

Figure (III.2) TG/ DTG curves of mixture M50C50 treated at heating rate of 30 °C/min.

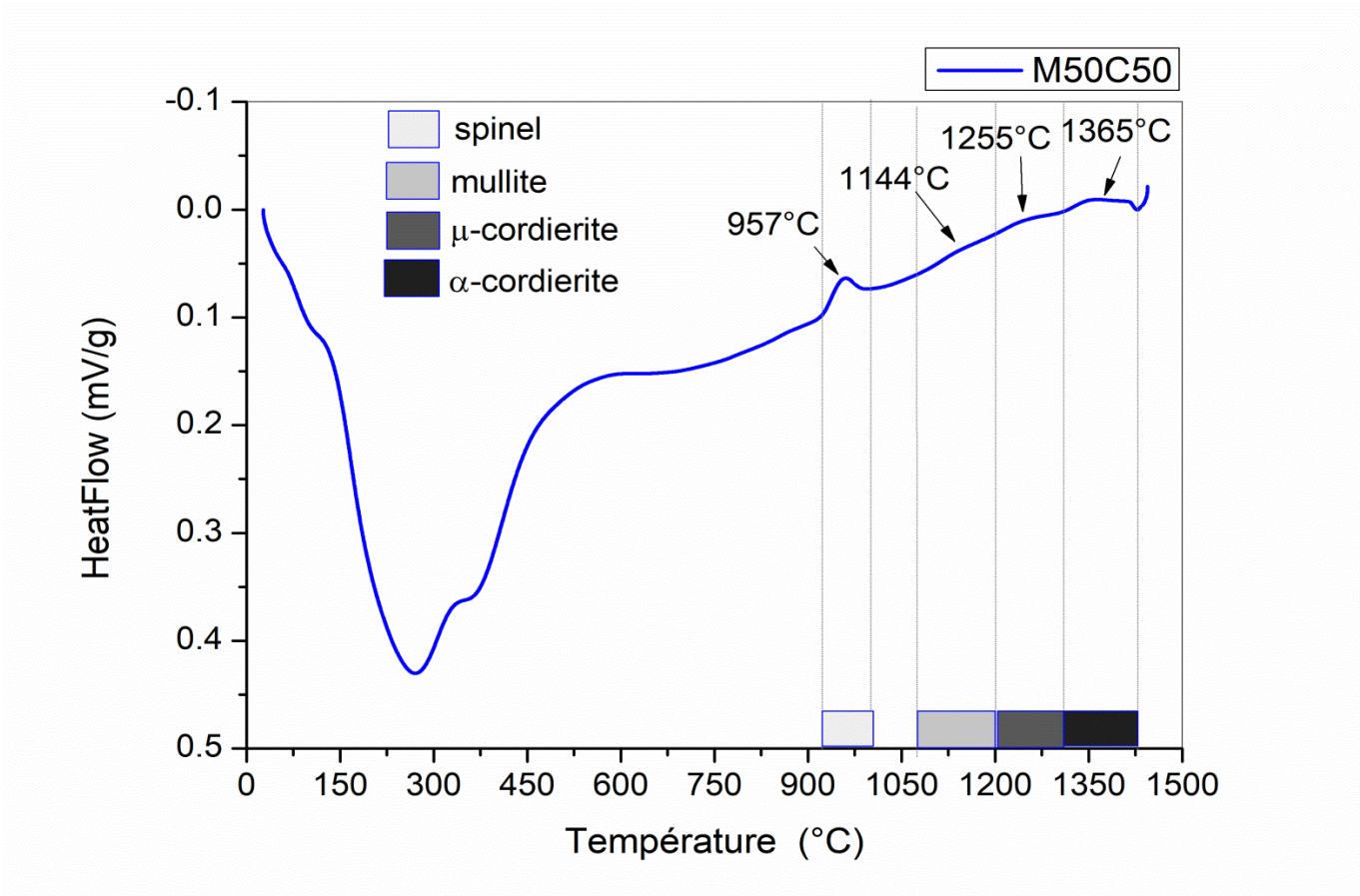

Figure (III.3) The DSC curves of M50C50 powder heated at 30 °C/min.

III.3 Analysis by DSC for M50C50

The results of the DSC for M50C50 powders that have been treated in several temperatures (910, 1000, 1095, 1185, 1260, 1320 and 1420 °C) in heating rate 30 °C/min, presented in Figure (III.4), which shows:

- ✧ In the 910 °C curve, there is no exothermic peaks appearing at this temperature, and all phase remain amorphous according to XRD results.
- ✧ An exothermic peak appears in the 1000 °C curve, and it is associated to formation of Al-Si spinel phase.
- ✧ The 1095°C curve indicates to the start of mullite phase formation which is confirmed by XRD results.
- ✧ The 1185 °C curve shows a small exothermic peak associated with Mg-Al spinel phase, same spinel were detected in XRD results.
- ✧ At 1260 °C curve, we can notice a new exothermic peak formed that is associated to

μ-cordierite phase as found in XRD results.

- ✧ An exothermal peak starts to form at 1320 °C curve that is related to α-cordierite phase formation.
- ✧ The last curve treated at 1420 °C indicate a fully formed exothermal peak that was related to α-cordierite phase

We used the results of DRX in Figure (III.4) to conform the DSC analysis results.

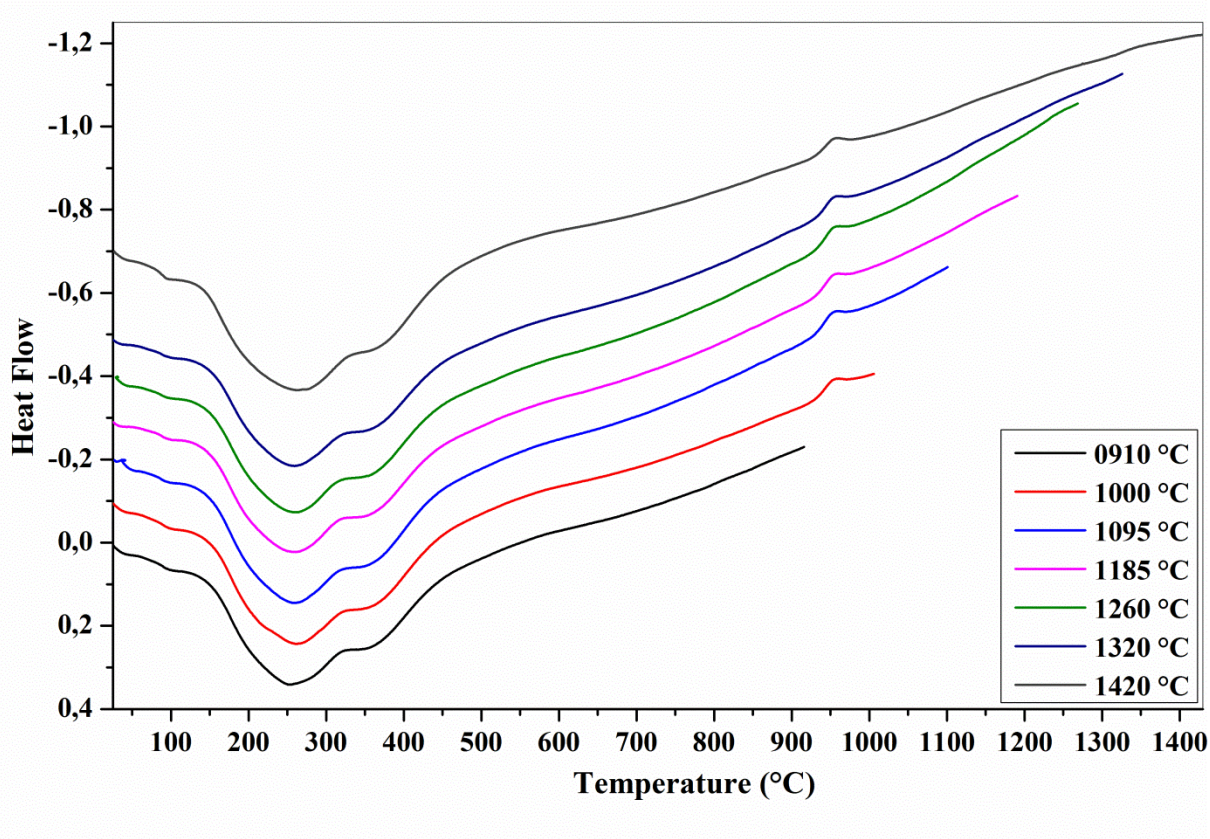

Figure (III.4) The DSC curves of M50C50 powder heated at 30 °C/min.

III.4 Analysis by XRD for M50C50

In order to determine the nature of all processes corresponding to the DSC peaks, and to characterize all crystalline substances that formed durning heating treatment, a M50C50 samples were treated in range of temperatures form 25 °C to 1450 °C, at heating rate 30 °C/min, then have been studied by X-ray diffraction. The X-ray diffractograms of the powders were calcined at 910 °C, 1000 °C, 1095 °C, 1185 °C, 1260 °C, 1320 °C and 1420 °C and presented in Figure (III.5).

It shows the following:

- ✧ The powders remain amorphous up to 1000 °C.
- ✧ At 1000 °C, Al-Si spinel phase is formed, and while increasing treatment temperature to 1095 °C, Al-Si spinel phase disappear and mullite ($Al_{4.80}Si_{1.20}O_{9.60}$) phase start forming, (this confirms the results of DSC curve peaks at 955 °C and 1132 °C).
- ✧ Mg-Al spinel phase ($Mg_{8.00}Al_{16.00}O_{32.00}$) is formed at 1185 °C and mullite phase peaks increased
- ✧ Both μ-cordierite ($Mg_{8.00}Al_{16.00}Si_{20.00}O_{72.00}$) and α-cordierite ($Mg_{4.00}Al_{8.00}Si_{10.00}O_{36.00}$) phase appear at 1260 °C along with decreasing in Mg-Si peaks.
- ✧ All mullite phase peaks are fully appeared at 1320 °C and μ-cordierite phase was transformed to α-cordierite completely.
- ✧ At 1420 °C, the Mg-Si spinel phase disappeared, and only mullite and α-cordierite phase was remained [10. 27-31].

We can notice that the TG /DTG and DSC analysis results are corroborated by the XRD analyses patterns results.

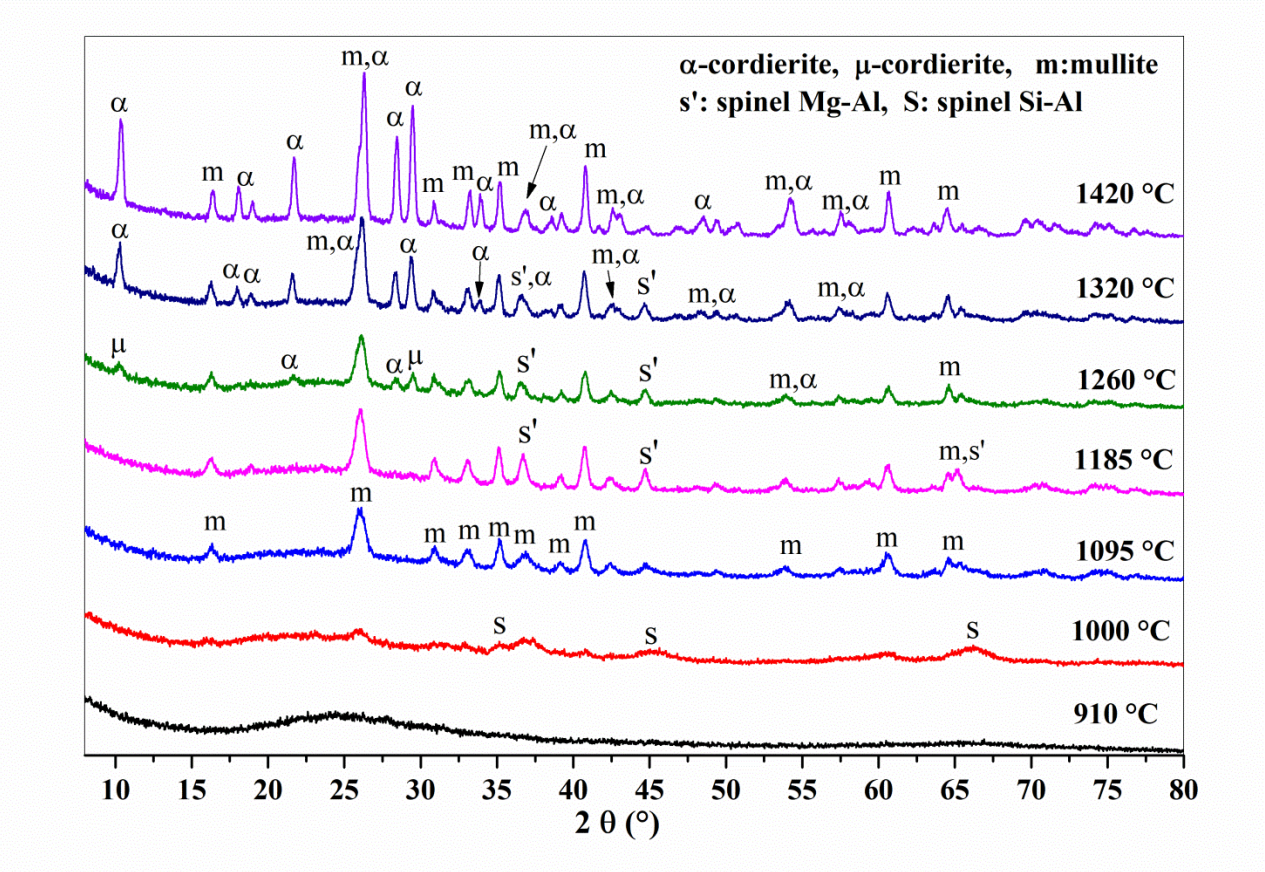

Figure (III.5) XRD curves of M50C50 powders heated at 30 °C/min.

III.5 Analysis by FTIR for M50C50

In order to identify all chemical compositions and bonds, a M50C50 powders that have been treated at different heating temperature by DSC

The results of FTIR spectroscopy of M50C50 composite obtained by DSC treatment are illustrated in Figure (III.6), shows:

- ✧ The characteristical pulsation at 1386 cm^{-1} is mainly due to Al-O bond vibrations in AlO4 quaternary for mullite in the mentioned composite, and by comparing it to pure mullite, its found that the vibrations shifted toward higher wave numbers, and the pulse become wider than the one in pure Mullite.
- ✧ As mentioned in some scientific resources, we have noticed that the bigger amount of cordierite in the composite, the narrower vibration range become which was explained by Mg dissolution in solid solution.
- ✧ The characteristic vibration at 1113.97 cm^{-1} belongs to Si-O cordierite bond, and the higher treatment temperature of composite get, the more we can notice a decrease in pulse intensity to become invisible in the composite, but there is also another pulse for SiO_4 structure (tetrahedral cordierite in the composite) at 828 cm^{-1}.
- ✧ The pulse found at 840.27 cm^{-1} correspond to different coordination's of Al, as for the one at 618.65 cm^{-1} its belong to Al bond vibrations in octagonal structure.
- ✧ Also the characteristical ranges for aluminum and magnesium spinal phase are invisible in the composite. [27, 19, 30, 32, 33].

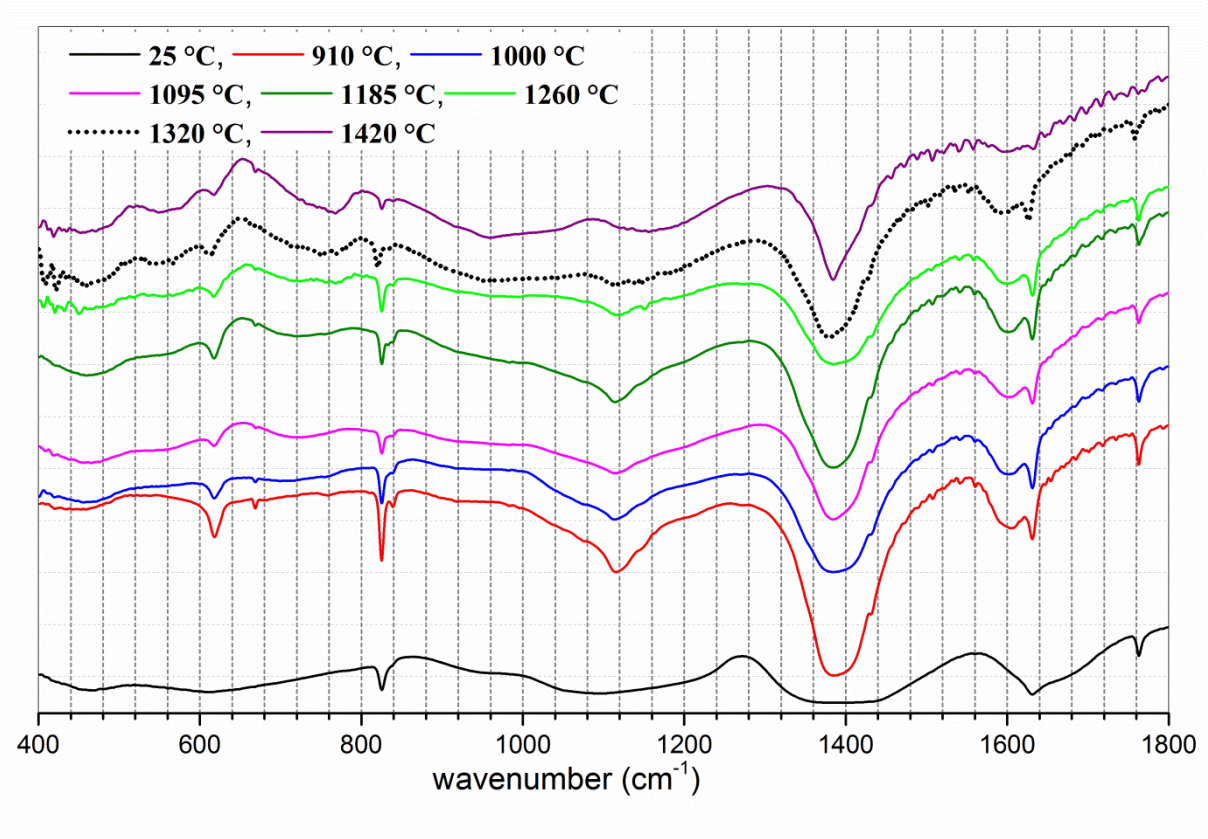

Figure(III.6) IR spectra of Mullite-Cordierite composite (M50C50) gel powders treated by DSC at different temperatures.

III.6 The thermal study of mullite-cordierite composites

III.6.1 The DSC analysis for MxxCyy

The thermal behavior of various Mullite-Cordierite composites with temperature were studied by DTA technique, the DSC curves for mullite-cordierite composites (M100C00, M95C05, M90C10, M85C15, M80C20, M50C50, M00C100) that have been treated from room temperature to 1430 °C at heating rate of 30 °C/min, are represented in Figure (III.7)

The DSC curve shows:

- ✧ Only two exothermic transformations which are associated to Al-Si spinel and mullite phase were formed durning the heat treatment for M100C00 up to M80C20, then other two transformations associated to μ-cordierite and α-cordierite phase were formed for M50C50.
- ✧ A decrease in the temperature of mullite phase formation from 1233 °C for M95C05 to

1144 °C for M50C50, we can say probably that the increase of cordierite ratio and the SiO_2 in mullite-cordierite composites can have a decreasing effect on the temperature that mullite phase form in.

- ✧ The endothermic transformation that corresponds to decomposition of magnesium nitrate can't be seen in M50C50, M85C15, M80C20.
- ✧ The Al-Si spinel phase is sharp and distinct in M100C00, M95C05 and M90C10, while it is diffused and broader in M85C15, M80C20 and M50C50 [19].

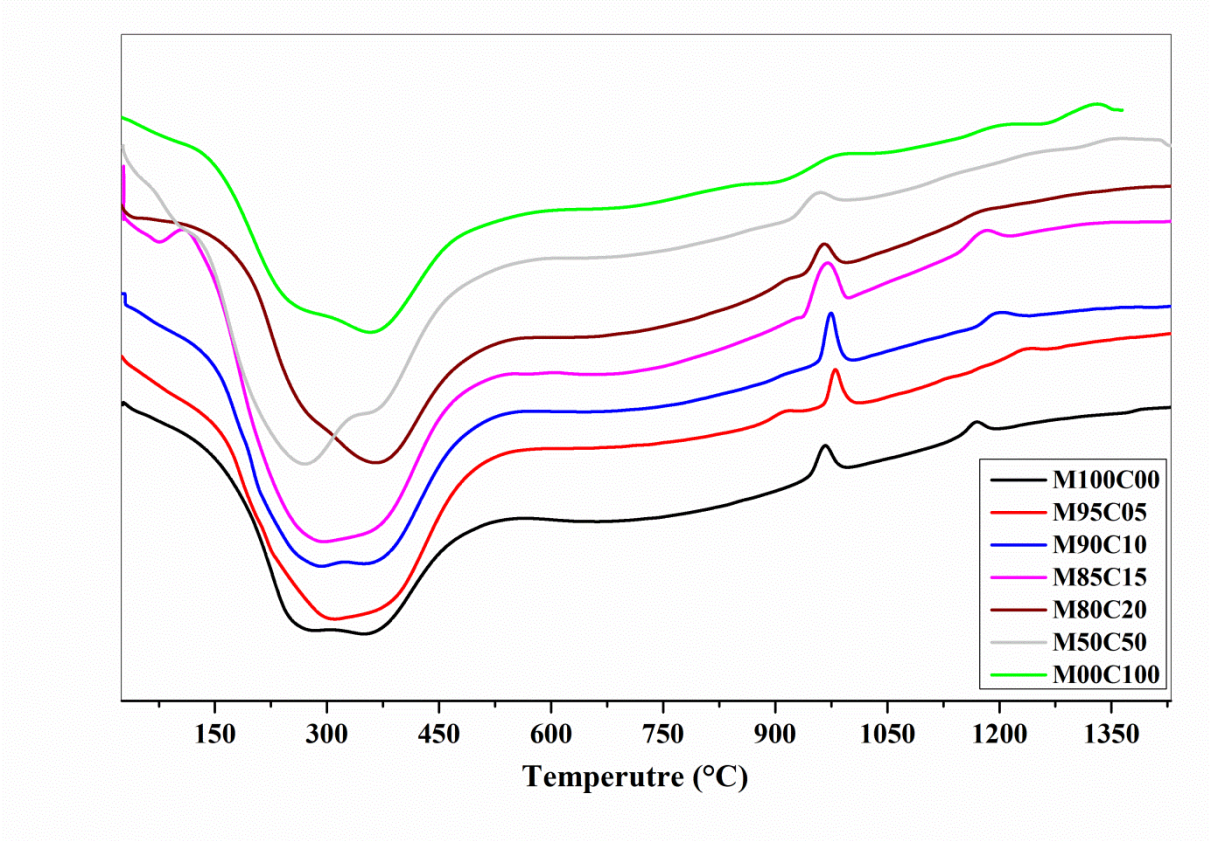

Figure (III.7) DSC curves of MxxCyy powder heated at 30 °C/min.

III.6.2 The XRD analysis for MxxCyy

In order to determine the differences in formed phases between various mullite-cordierite composites, a calcination to the equivalent powders of mullite-cordierite composites (M100C00, M95C05, M90C10, M85C15, M80C20, M50C50, M00C100) were carried out at temperatures between 1350 °C and 1430 °C in heating rate 30 °C/min by DSC. The X-ray diffractograms of these powders are presented in Figure (III.8).

We can see the following:

- ✧ Only single phase mullite was observed in M95C05 at temperature above 1450 °C with an increase in peaks intensity compared to M100C00.
- ✧ both composites M90C10 and M85C15 formed Mg-Al spinel phase as well as less intense mullite phase, meanwhile M80C20 showed an additional peak indicating the start of α-cordierite phase formation.
- ✧ Only two fully formed phases mullite and α-cordierite were observed in M50C50 [19, 31, 33].

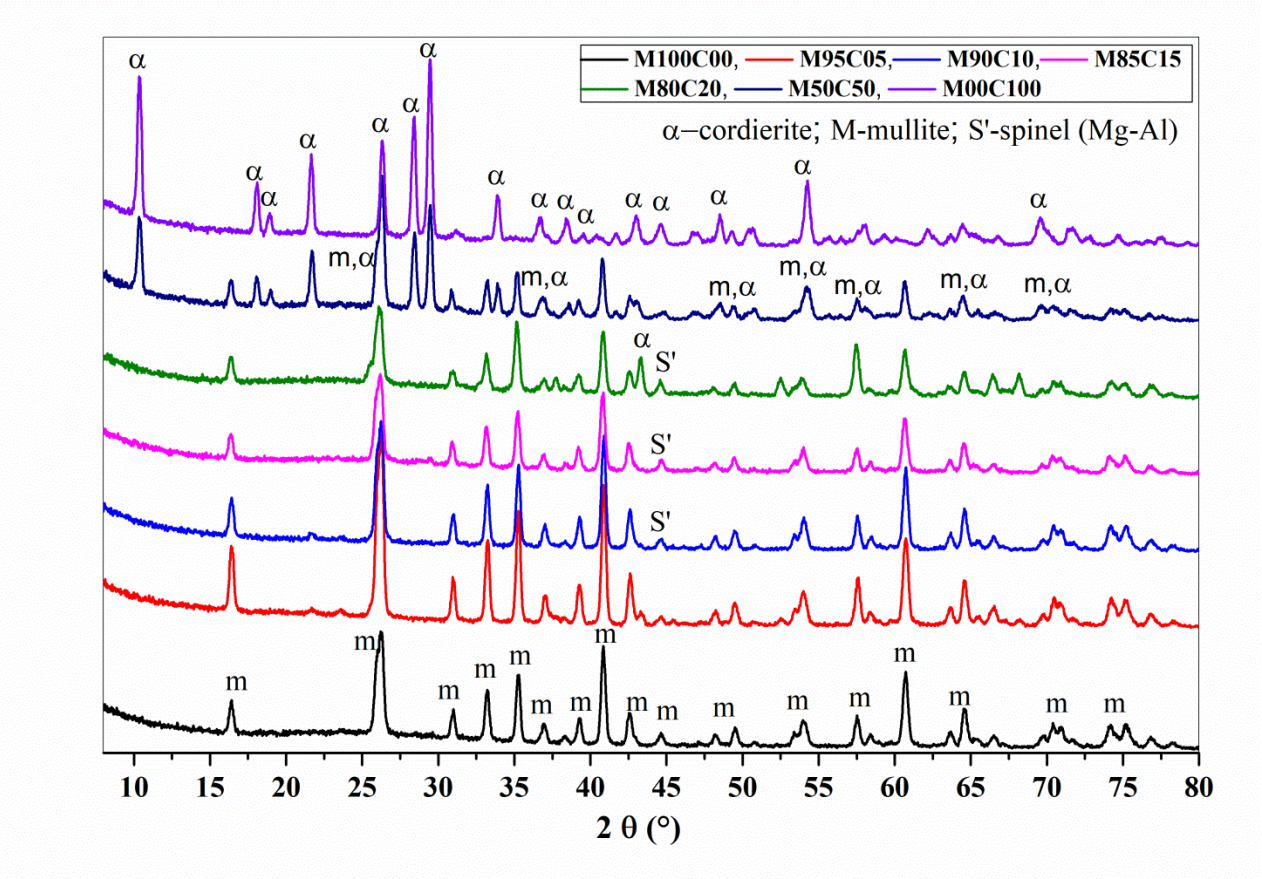

Figure (III.8) XRD curves of MxxCyy powder heated at 30 °C/min.

III.7 Activation Energy

III.7.1 Activation Energy of Al-Si spinel formation for M50C50 using DSC

III.7.1.1 Non-isothermal treatment

The non-isothermal activation energy for Al-Si spinel formation was calculated using Kissinger, Boswell, and Ozawa methods according to the equations shown below:

Ozawa equation: $\ln(\varphi) = -1.0518\frac{E_a}{RT_p} + C$ **(1)**

Boswell equation: $\ln\left(\frac{\varphi}{T_p}\right) = -\frac{E_a}{RT_p} + C$ **(2)**

Kissinger equation: $\ln\left(\frac{\varphi}{T_p^2}\right) = -\frac{E_a}{RT_p} + C$ **(3)**

The Figure (III.9) represent the exothermic peak for Al-Si spinel formation in DSC curves, that occurs without weight loss, and treated between 900 °C to 1075 °C in various heating rate (20, 30, 40, 50 °C/min), after defining the maximum temperature T_P of each heating rate peak , it show that :

- ✧ The maximum temperature T_P value of the exothermic peak shift to higher temperature (from 947.46 °C to 966.01°C) as the heating rate increases from 20 °C/min to 50 °C.

In order to calculate the activation energy to the exothermic peak for Al-Si spinel formation, the equations 1, 2, 3 were used, Figure (III.10) represent the plots of Y versus (1/Tp) of spinel formation at various heating rates. The values of the activation energy E_a and R^2 for Al-Si spinel phase are presented in Table (III.1), and it shows that:

- ✧ The activation energy of Kissinger, Boswell and Ozawa methods are found to be 595.64KJ/mol, 605.86 KJ/mol and 585.74 KJ/mol respectively.

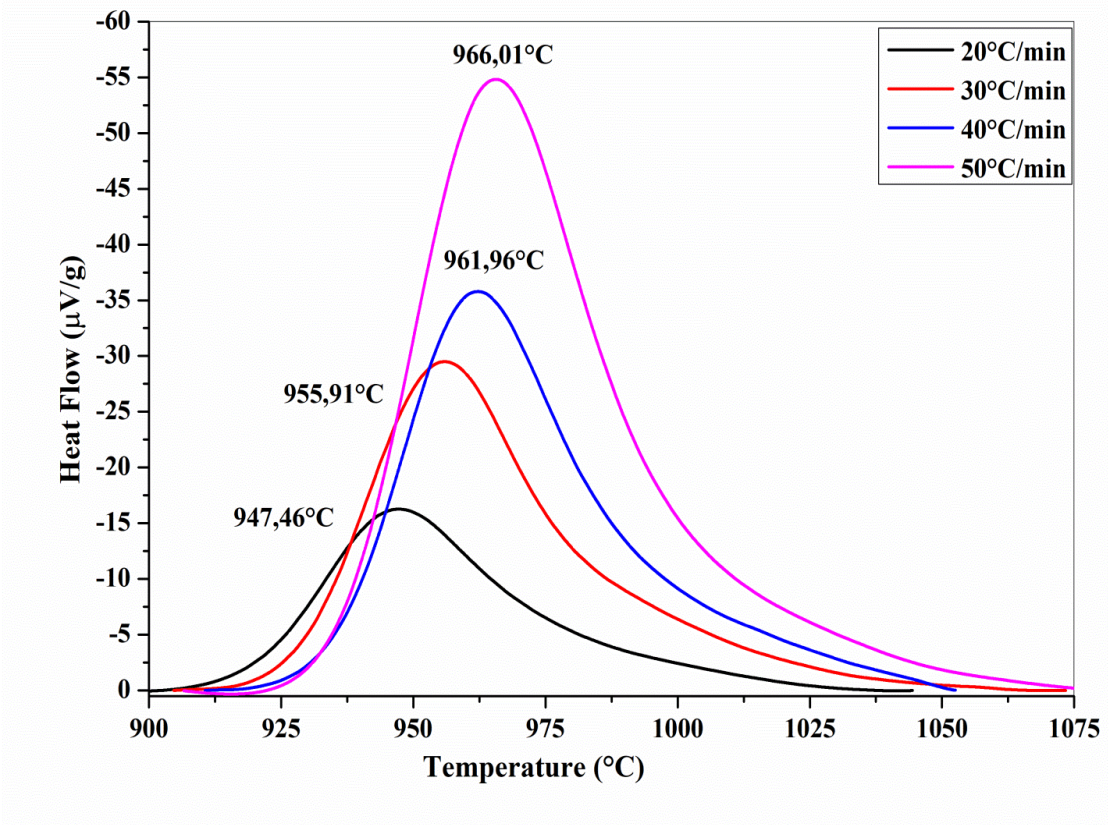

Figure (III.9) the DSC curve for M50C50 treated powder between 900°C to 1075°C in various heating rate.

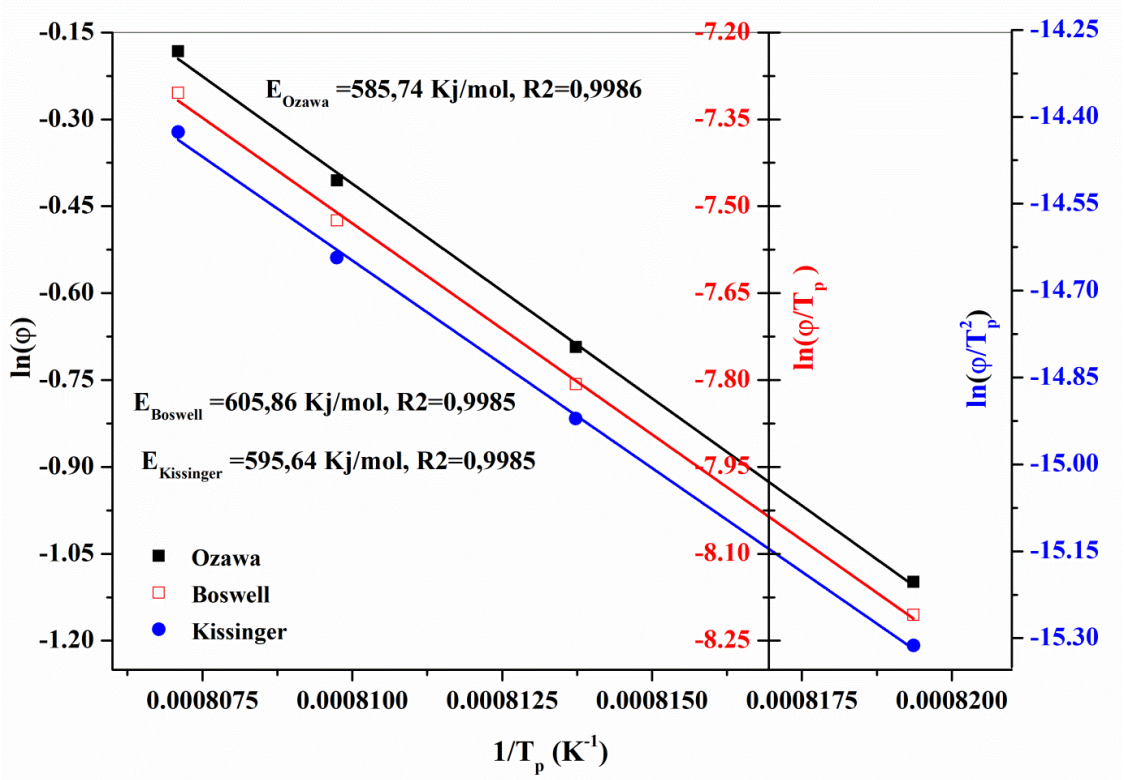

Figure (III.10) Plots of Y versus (1/Tp) of spinel formation at various heating rates.

Table (III.1) The values of E_a, R and R^2 for spinel phases.

Method	Ea (KJ/mol)	R	R^2
Ozawa	585.74	-0.99953	0.99860
Boswell	605.86	-0.99952	0.99856
Kissinger	595.64	-0.99950	0.99851

Calculation of n

The value of the Avrami parameter n, which indicates the crystallization mode, was calculated using the following equation:

$$n = 2.5\frac{T_p^2}{\Delta T\frac{E_a}{R}} \quad \text{..... (4)}$$

The results of calculation are presented in Table (III.2).

Table (III.2) The value of the Avrami parameter n for spinel phase.

V	Tp (K)	ΔT(K)	n	n_{moy}
20	1220.46	38.83182	1.10	1.14
30	1228.91	37.23981	1.17	
40	1234.96	37.54031	1.17	
50	1239.01	39.314462	1.12	

Calculation of m

The value of the kinetic parameter m, which indicates the dimensionality of crystal growth, was calculated using the Matusita equation (Kissinger modified equation)

Matusita equation: $\ln\left(\frac{\varphi^n}{T_p^2}\right) = -\frac{mE_a}{RT_p} + c$ **.....(5)**

The Figure (III.11) represents the plot of $\ln\left(\frac{\varphi^n}{T_p^2}\right)$ versus 1/Tp according to Matusita equation, Along with Table (III.2), we can note the following:

✧ According to Matusita equation, the parameter **m** was found to be **1.15**, and according to

equation 4, the parameter $\mathbf{n}_{moy}$ was found to be **1.14,** these values are close to **1.5**.

- ✧ We can conclude that the crystallization mode and the dimensionality of crystal growth of the exothermic peak for Al-Si spinel phase during formation is probably three dimensional (polyhedron) diffusion [26].

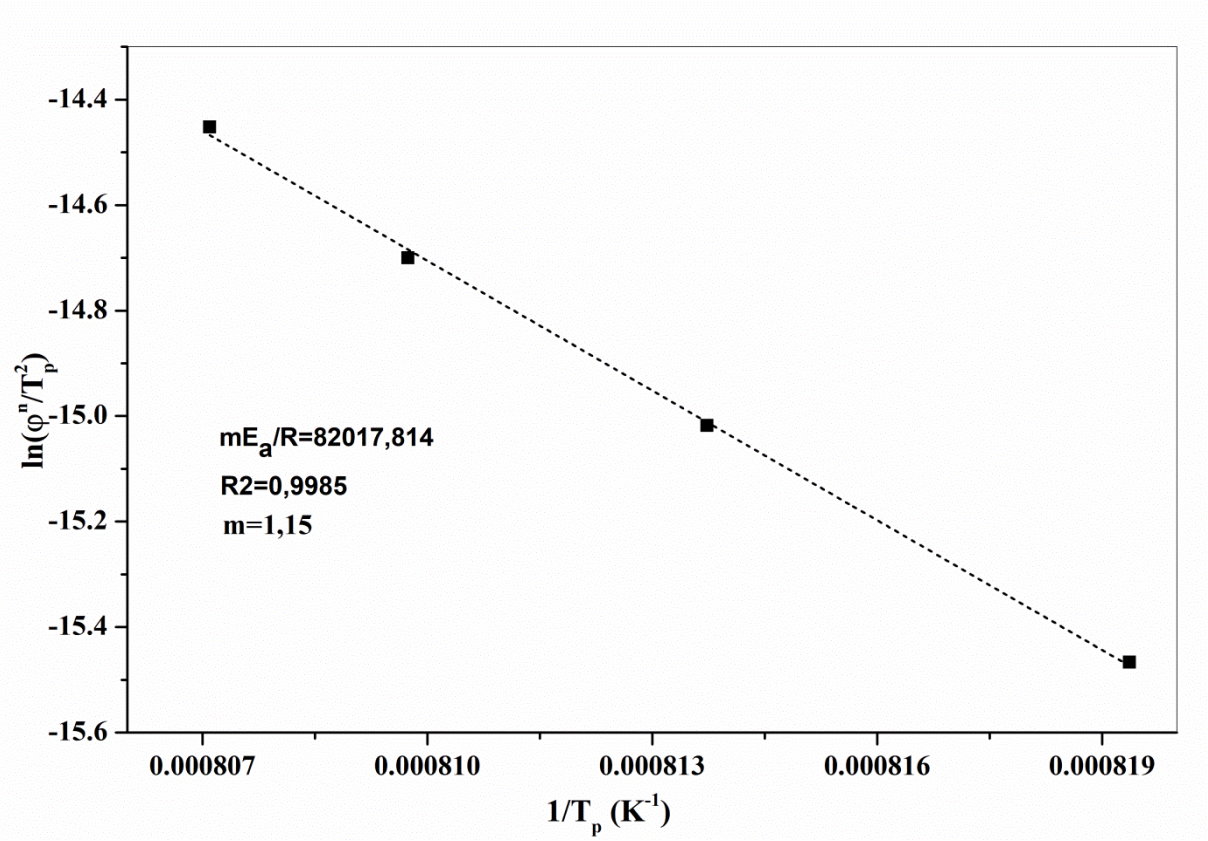

Figure(III.11) Plot of $\ln\left(\frac{\varphi^n}{T_p^2}\right)$ versus 1/Tp according to Matusita equation.

III.7.1.2 Isothermal treatment

The Figure (III.12) show the variation of the crystallized fraction of the exothermal peak for Al-Si spinel phase under different heating rate, which was determined from the DSC results.

- ✧ We can notice that the crystallization fraction x at a temperature T differs for 20, 30, 40, 50 °C/min.

The Figure (III.13) shows the rate of spinel growth with time under different heating rates, we can recognize the following:

- ✧ A decrease in time of the spinel growth rate from 6 min: 40 s in heating rate 20 °C/min

to 3 min: 20 s in heating rate 50 °C/min.

✧ An increase in the spinel growth rate from 0.007 s^{-1} in heating rate 10 °C/min to 0.018 s^{-1} in heating rate 50 °C/min.

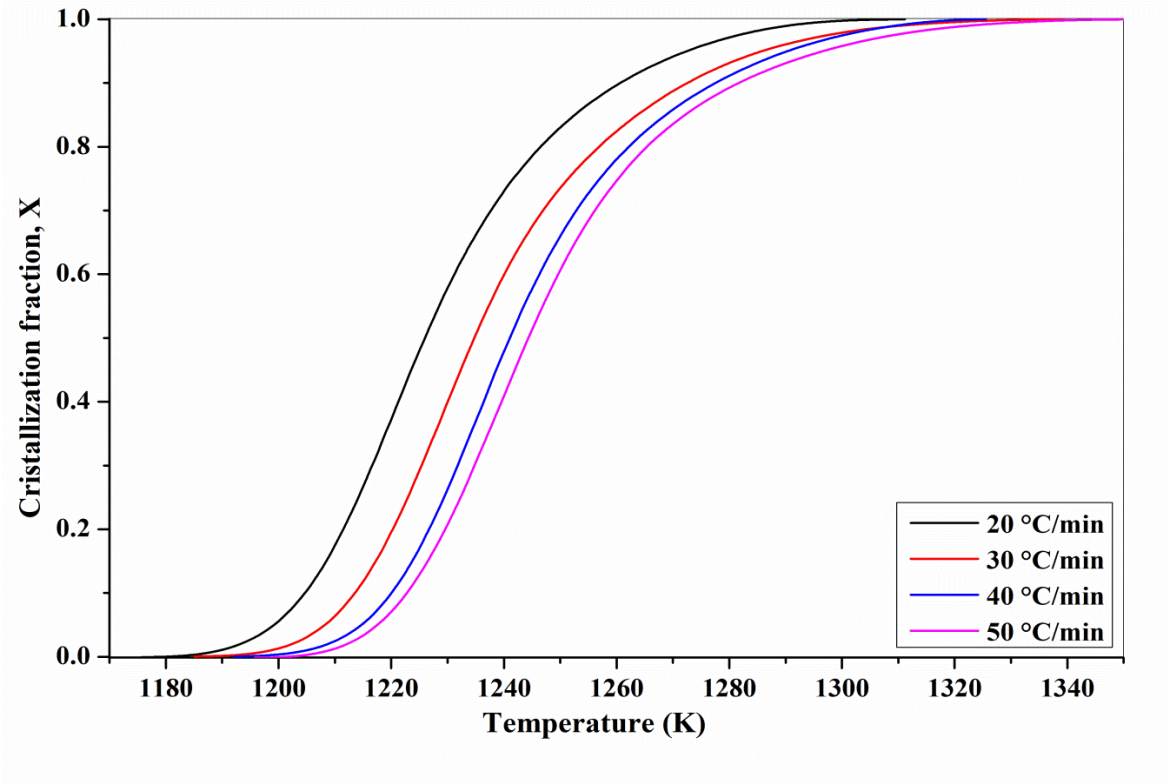

Figure (III.12) the variation of the crystallized fraction of Al-Si spinel phase with time for M50C50 under different heating rate.

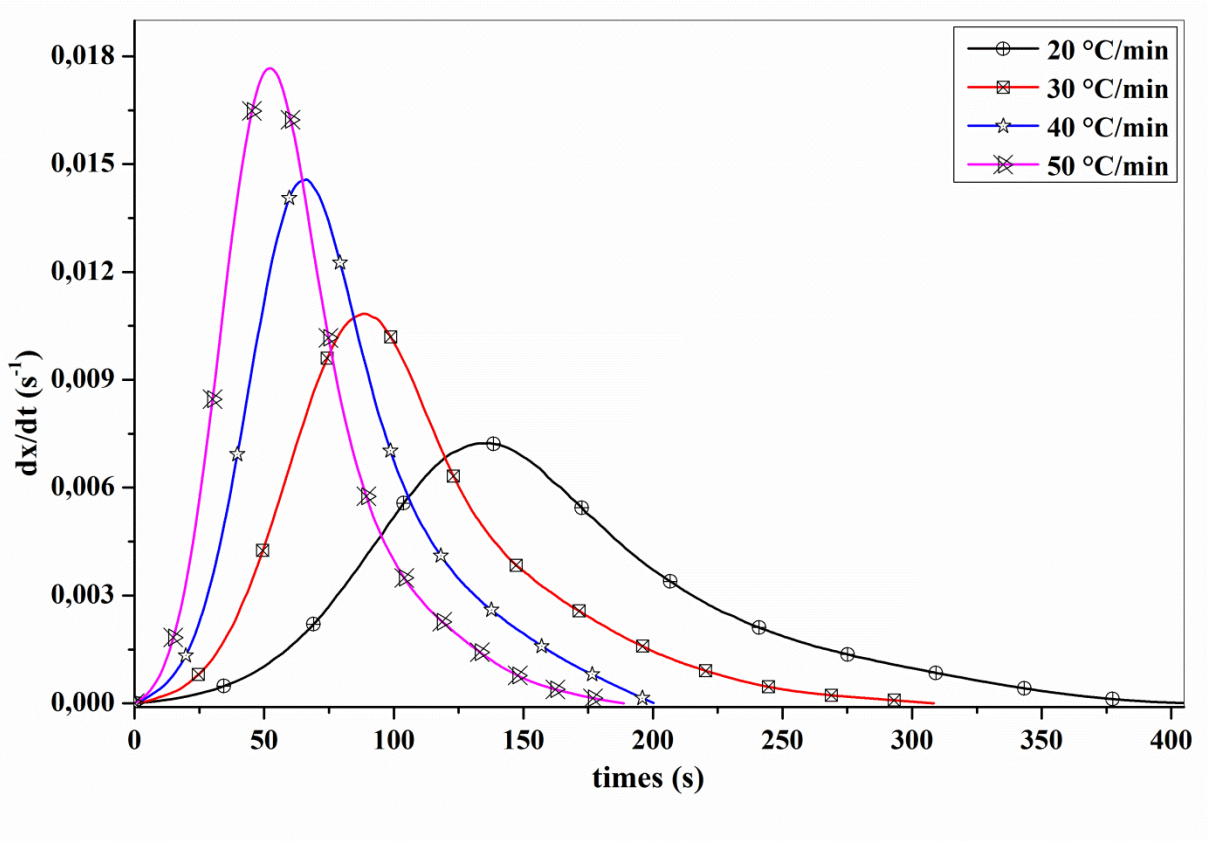

Figure (III.13) The rate of spinel growth with time for M50C50 under different heating rates.

Figure (III.14) presents the plot of ln(dx/dt) and 1/T versus crystallized fraction x at different heating rates from DSC experiment. A mathematical method through non-isothermal techniques was proposed by LIGERO et al [34]. If the same value of crystallized fraction x in every experiment at different heating rates is selected, the function ln(dx/dt) versus 1/T gives a linear curve (III.15). The activation energy can be calculated from the slope of the function ln(dx/dt)=f(1/T), the values of activation energy E_a for different crystallized fractions, are listed in Table (III.3). The coefficient of determination R^2 is greater than 0.99 for different x values, and the average activation energy of spinel formation is 605.86 KJ/mol, which is an good agreement with that of 595.64 KJ/mol estimated by non-isothermal DSC treatment. Once the activation energy is known, the value of $\ln[k_0 f(\varkappa)]$ can be calculated, Figure (III.16) Plot of $\ln(k_0 f(x))$ versus crystallization fraction x for composite mullite-cordierite heated at a heating rate of 20 °C min^{-1}. The Avrami parameter **n**, was determined by the selection of many pairs of x_1 and x_2 that satisfied the condition $\ln[k_0 f(\varkappa_1)] = \ln[k_0 f(\varkappa_2)]$, and the average values of n for each heating rate are listed in Table (III.4).

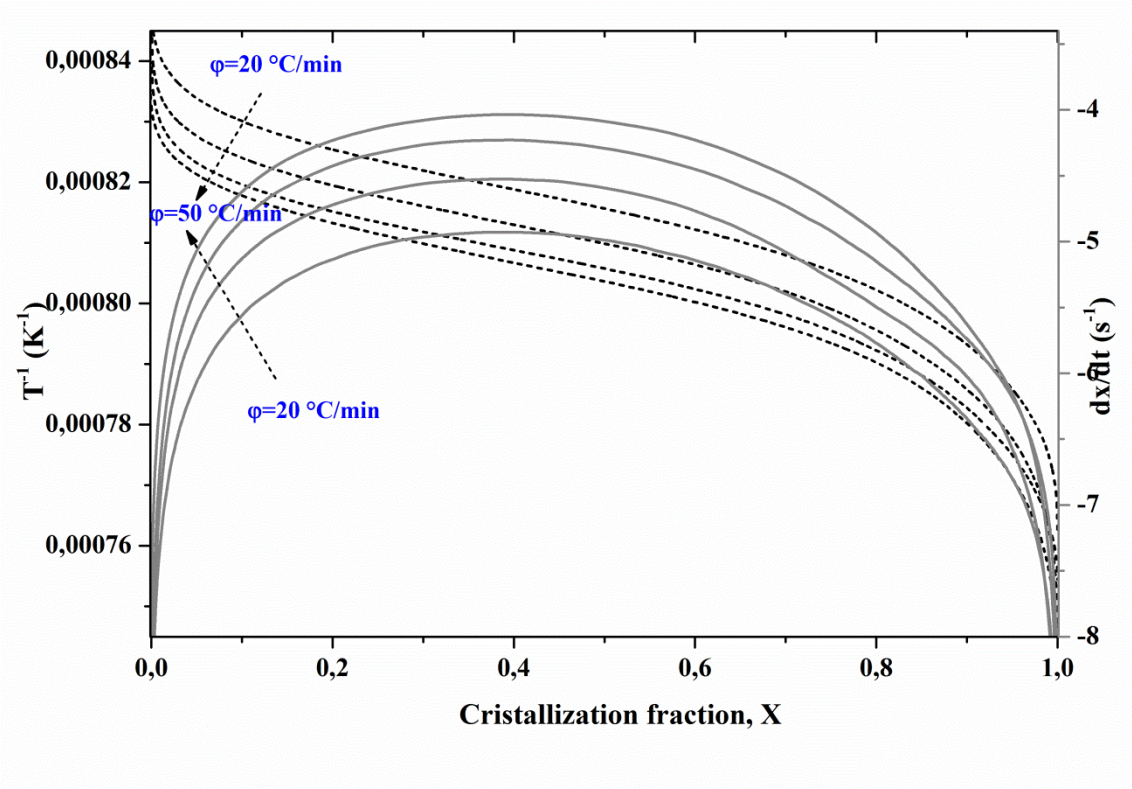

Figure (III.14) Plot of ln(d*x*/d*t*) and 1/*T* versus of crystallized fraction x at different heating rates.

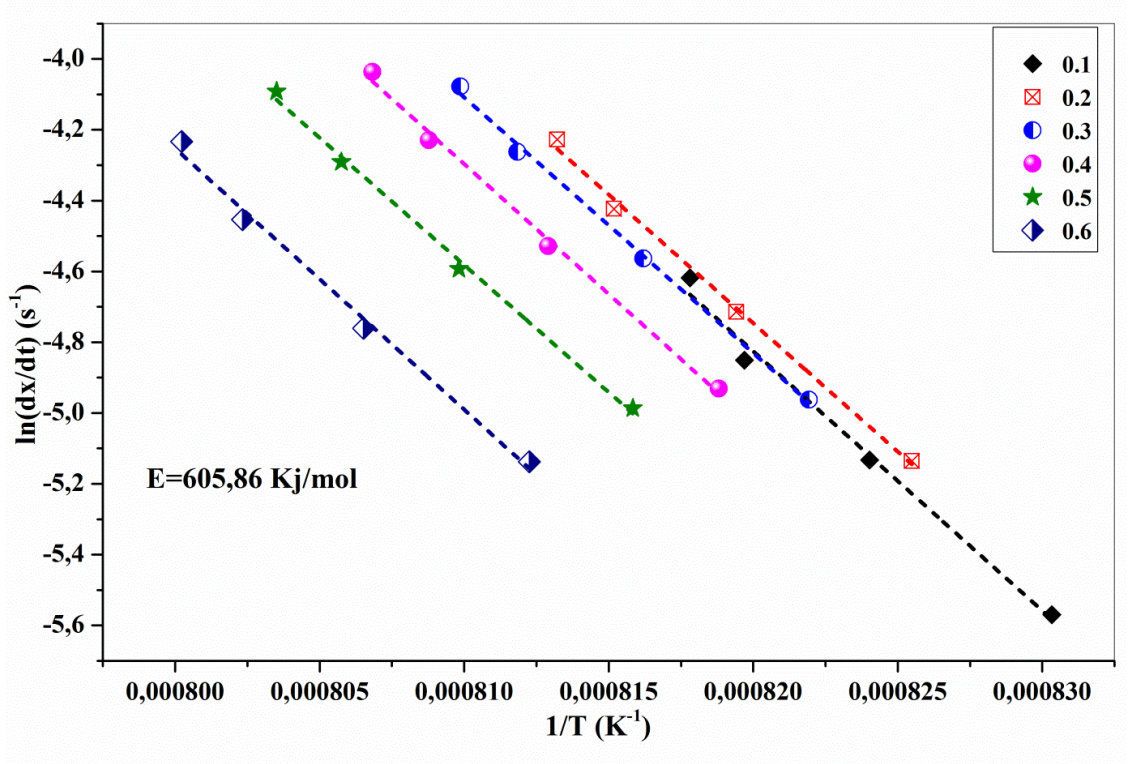

Figure (III.15) Plots of ln(dx/dt) versus 1/T at same value of crystallized fraction x at different heating rates.

Table (III.3) Values of the activation energy E_a for different values of crystallized fraction.

X	slop	R	R^2	E(j/mol)	E(Kj/mol)
0.1	-73295.2701	**-0.99522**	**0.9857**	609376.8759	**609.38**
0.2	-72573.3224	**-0.99827**	**0.99482**	603374.6024	**603.37**
0.3	-72233.6534	**-0.99892**	**0.99676**	600550.5941	**600.55**
0.4	-73499.2573	**-0.99809**	**0.99426**	611072.8254	**611.07**
0.5	-71898.8873	**-0.99831**	**0.99492**	597767.3487	**597.77**
0.6	-73734.9986	**-0.99651**	**0.98956**	613032.7783	**613.03**

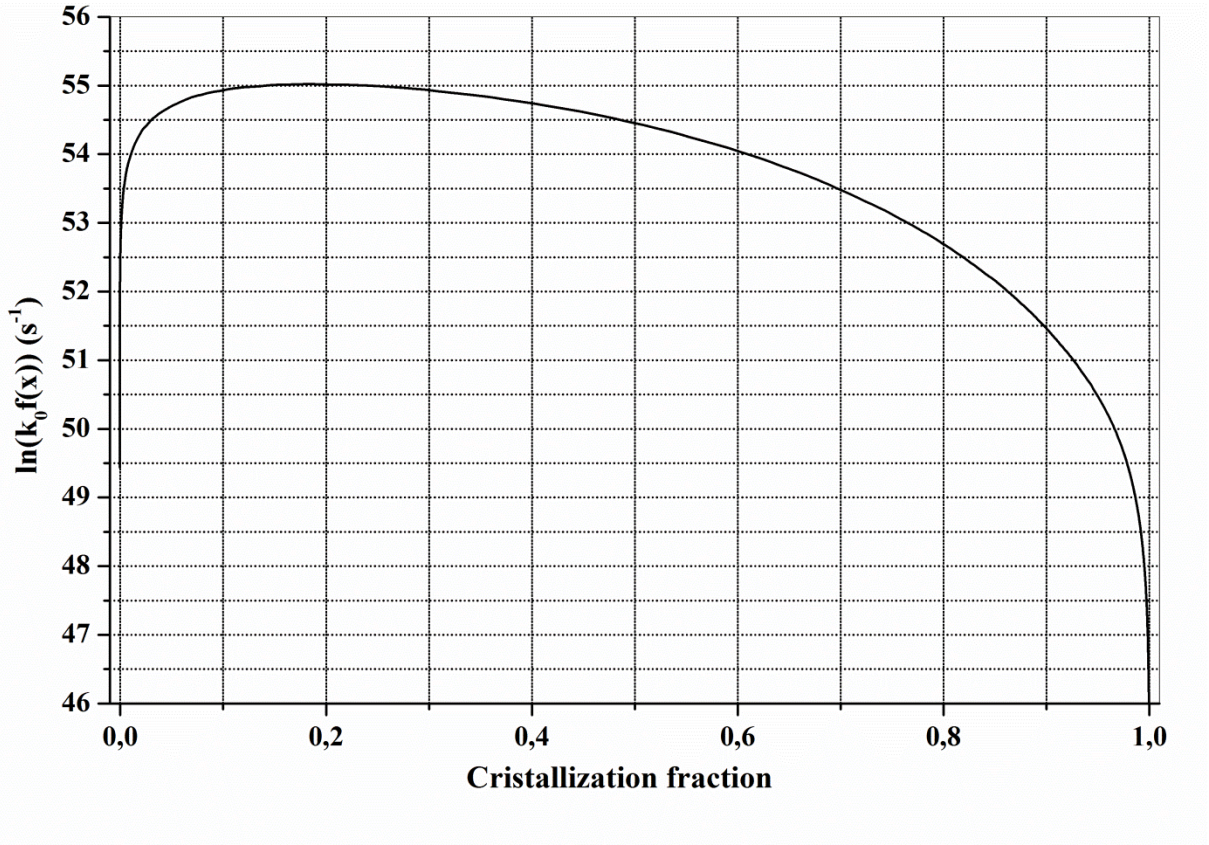

Figure (III.16) Plot of $\ln(k_0 f(x))$ versus crystallization fraction x for composite mullite-cordierite heated at a heating rate of 20 °C min^{-1}.

Table (III.4) Values of Avrami parameter and frequency factor at different heating rates.

ϑ(°C/min)	n	$K_0/ 10^{23}$ (s^{-1})
20	1.26	4.246
30	1.27	3.32
40	1.28	3.9
50	1.24	3.55
	n_{moy}= 1.26	**K_{0moy}= 3.754x10^{23} (s^{-1})**

According to Table (III.4), the value of the average Avrami parameter $\mathbf{n}_{moy}$ is **1.26**, this value is close to 1.5, which suggests that the crystallization process of Al-Si spinel phase in mullite-cordierite should be controlled by diffusion. The value of the kinetic parameter **m** was calculated by the same method in the non-isothermal treatment, Figure (III.17) shows the plot of $\ln\left(\frac{\varphi^n}{T_p^2}\right)$ versus 1/Tp according to Matusita equation, and **m** was found to be **1.24**, which suggests a three-dimensional growth of Al-Si spinel phase crystal in mullite-cordierite composite [26]. The value of **m** and **n** are close to **1.5** which is compatible with the non-isothermal treatment results.

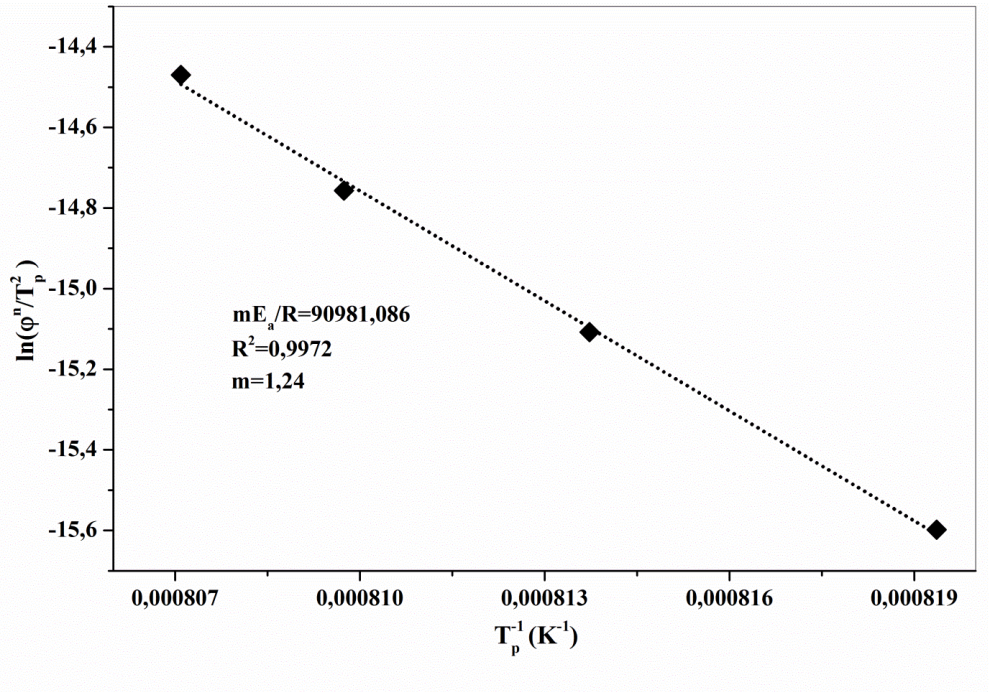

Figure (III.17) Plot of $\ln\left(\frac{\varphi^n}{T_p^2}\right)$ versus 1/Tp according to Matusita equation.

Conclusion

Conclusion

The objective of this work is to prepare Mullite-Cordierite composites by Sol-Gel method using raw materials such as Aluminum nitrate nonahydrate, Magnesium nitrate hexahydrat and TEOS, and to analyse phases transformation behavior that accurse during thermal treatment, also to measure the activation energy and Avrami parameters in both isothermal and non-isothermal treatments.

The results of this study showed that:

- ✧ The thermal analyse performed by TG/DTG, DSC and DIL for M50C50 conforms the formation of Al-Si spinal phase at 957°C along with mullite at1144°C , μ-cordierite at 1255° and α-cordierite phase at1365°C, also the XRD analysis.
- ✧ The activation energy was calculated from the exothermic Al-Si spinal peak by DSC, in the case of isothermal and non-isothermal treatments, it was around 605.86 KJ/mol and 595.64 kJ mol^{-1} respectively, also the Avrami parameter n and the numerical factor m are close to 1.5, indicating the crystallization mode and the dimensionality of crystal growth of the exothermal peak for Al-Si phase during formation as three dimensional (polyhedron) diffusion.
- ✧ The thermal analyse performed by DSC for MxxCyy, conforms the effect of increasing cordierite ratio on mullite formation temperature by decreasing it, also that the cordierite phase can only form above 15 % by it weight in MxxCyy composites.

REFERENCES

1. M. Fazeli, J. P. Florez and R. A. Simão, "Improvement in adhesion of cellulose fibers to the thermoplastic starch matrix by plasma treatment modification", Composites Part B: Engineering. Volume 163 (2019) 207-216.

2. R. Elhajjar, Valeria La Saponara and Anastasia Muliana, "Smart Composites: Mechanics and Design (Composite Materials)", CRC Press, (2013).

3. Felix Singer, Sonja S. Singer, "Industrial Ceramics", London, p 482, (1984).

4. M. D. Karkhanavala, F. A. Hummel, "The Polymorphism of Cordierite", J. Am. Ceram. Soc., 36 [12] (1953) 389-392.

5. Nadjet Aklouche, "Preparation et etude des Composes Cordierite et Anorthite", Thése de doctorat, 2009, P.70.

6. Bin, Tang, YouWei Fang, ShuRen Zhang and HaiYan Ning, "Preparation and characterization of cordierite powders by water-based sol-gel method", Indian Journal of Engineering and Materials Sciences, 18 (2011) 221-226.

7. A. Chowdhury, S. Maitra, H. S. Das, A. Sen, G. K. Samanta and P. Datta, "Synthesis, Properties and Applications of Cordierite Ceramics", InterCeram International Ceramic Review, 56 (2007) 98-102.

8. Redaoui Djaida, "Étudier le mécanisme des transformations de phase des matériaux réfractaires préparés à partir d'oxyde de magnésium local et de kaolinite", Thése de doctorat, 2018, P.26.

9. A. Askin, İ. Tatar, Ş. Kılınç and Ö. Tezel, "The Utilization of Waste Magnesite in the production of the Cordierite Ceramic", Energy procedia, 107 (2017) 137-143.

10. N. M. El-Buaishi, I. Janković-Častvan, B. Jokić, D. Veljović, D. Janaćković, R. Petrović, "Crystallization behavior and sintering of cordierite synthesized by an aqueous sol–gel route", Ceramics International, 38 (2012) 1835-1841.

11. J. F. Shockelford and R. H. Doremus, " Ceramic and Glass Materials: structure, properties and processing", New York ,P.27-35, (2008) .

12. H. Schneider, S. Komarneni, "Mullite", Weinheim, P.1-14,149-151,313-322, (2006).

13. Philippe Boch, Jean Claude Niépce, "Ceramic Materials : Processes, Properties and Applications", United States, P.214-205,(2007).

14. I. Stefaniuk and I. Rogalska, "EMR study and superposition model analysis of Cr3+ and Fe3+ impurity ions in mullite powders used in aerospace industry",

NUKLEONIKA; 60 (3) (2015) 399−403.

15. Ahmed Esharghawi, "Élaboration de matériaux poreux à base de mullite par procédé SHS", 2009, P.9.

16. D. Thomas., Ceramic Engineering and Science Proceedings", Published by The American ceramic Society, P.1, (1993).

17. D. P. H. Hasselma and J. R. Thomas, "Thermal Conductivity 20", Virginia, P.119, (1989).

18. John B. Wachtman, "Fabrication of Ceramics: Ceramic Engineering and Science Proceedings", Hoboken, P.7, (2009).

19. Mohamed G. M. U. Ismail, H. Tsunatori, and Z. Nakai, "Preparation of Mullite Cordierite Composite Powders by the Sol-Gel Method: Its Characteristics and Sintering ", J. Am. Ceram. Soc ,73, 31(1990) 537-43.

20. Ankita Bilung, "Synthesis and Characterization of Cordierite-Mullite Composite", Nation Institute of technology, Diploma 2012, P.10.

21. Allen M. Alper, "Phase Diagrams In Advanced Ceramics", San Diego, P.45, (1995).

22. S. Aramaki and R. Roy, "Revised Phase Diagram for the System Al2O3-SiO2", J. Am. Ceram. Soc., 45(1962) 229-242

23. V. Raghavan, "Materials Science and Engineering", New Delhi, P.163, (2011).

24. In-Ho Jung, Sergei A. Decterov, Arthur D. Pelton ., Critical thermodynamic evaluation and optimization of the CaO–MgO–SiO2 system., Journal of the European Ceramic Society 25 (2005) 313–333

25. Tibor Gasparik, "Phase Diagrams for Geoscientists", Springer Science+Business Media New York 2003, 2014.

26. M. Romeo, J. Martín-Márquez, J. Ma. Rincón, "Kinetic of mullite formation from a porcelain stoneware body for tiles production", J. Euro. Ceram. Soc., 26 (2006) 1647-1652.

27. I. Jankovic Castva, S. Lazarevic´, D. Tanaskovic´, A. Orlovic´, R. Petrovic´and Dj. Janac´kovic, " Phase transformation in cordierite gel synthesized by non-hydrolytic

sol–gel route “,Ceramics International, 33 (2007) 1263–1268.

28. P. Padmaja, G. M. Anilkumar, P. Mukundan, G. Aruldhas and K. G. K. Warrier, “ Characterisation of stoichiometric sol–gel mullite by fourier transform infrared spectroscopy “, International Journal of Inorganic Materials, 3(2001) 693–698.

29. G. Shcherbakova and A. Pokhorenko, “Synthesis of Preceramic Organomagnesium Oxanealumoxane Siloxanes “,The 23rd International Electronic Conference on Synthetic Organic Chemistry, 41, 52 (2019). 1-12.

30. L. T. Jurado, R. M. Arévalo Hernández, and E. Rocha-Rangel, “ Sol-Gel Synthesis of Mullite Starting from Different Inorganic Precursors “, Journal of Powder Technology, 10 (2013)1155.

31. R. Gop Chandran, K. C. Patil and G. T. Chandrappa, “ Combustion Synthesis, Characterization, Sintering and Microstructure of Mullite-Cordierite Composites “ , Journal of materials science letters, 14 (1995) 548-551.

32. T. Gonzalez-Carreno, Sobrados, and J. Sanz “ Formation of Mullite and Spinel Phases from SiO2-Al2O3 Gels Prepared by a Spray Pyrolysis Technique. A 29Si and 27Al MAS NMR Study “,Chem. Mater,19 (2007) 3694-3703.

33. P. P tacer, F. Soukal, T. Opravil, M. Noskova , J. Havlica and J. Brandstetr, “ Mid-infrared spectroscopic study of crystallization of cubic spinel phase from metakaolin “, Journal of Solid State Chemistry 184 (2011) 2661–2667.

34. R. A. LIGERO, J. VAZQUEZ, P. VILLARES, R. JIMENEZ-GARAY, study of the crystallization kinetics of some Cu−As−Te glasses. Journal of Materials Science, 26 (1991) 211−215.

الملخص

تم تحضير مركب الميليت – كورديريت بطريقة المحاليل الهلامية، و ذلك باستخدام مسحوق نترات المغنيسيوم ومسحوق نترات الالومنيوم ومحلول تيترايثيل أورثوسيليكات كمواد أولية ، أين تم خلط هذه المواد بنسب مختلفة حسب الصيغة الستكيومترية للمركب المراد الحصول عليه، و لتحليل المواد المحضرة استخدمنا عدة تقنيات في التحليل منها التحليل الحراري الكتلي والتحليل الحراري التفاضلي TG/DSC، وكذا التحليل بواسطة مقياس التمدد الحراري (Dilatometry) وهذا لأجل مراقبة التحولات الطورية، و لتأكيد ذلك استخدمنا تقنية التحليل بواسطة حيود الاشعة السينية (XRD) و التي بها تم معرفة الأطوار المتشكلة في المركب M50C50 و هي الميليت و الكورديريت، كما تتبعنا مراحل التحول الطوري للمساحيق M50C50 المعالجة بواسطة DSC عند مختلف درجات الحرارة بتقنية التحليل بواسطة الاشعة تحت الحمراء (FTIR) ، أين استطعنا بواسطة نطاقات الاهتزاز ان نتعرف على الأطوار المتشكلة بمختلف درجات الحرارة و خاصة الأطوار غير المتبلورة، كما تم حساب طاقة التنشيط ومعاملات أفرامي للنمو والتنوي لطور السبينال Al-Si في حالة تغير درجة الحرارة و ثبوتها باستخدام نتائج التحليل الحراري التفاضلي، اين تحصلنا على قيم الطاقة التالية: 595.64 Kj/mol و 605.86 Kj/mol على الترتيب، أما قيمة معاملات النمو المرفولوجي n و m فهي تقارب 1.5 مما يشير إلى أن حجم التنوي السائد في تشكل طور سبينال متبوعا بنمو ثلاثي الأبعاد لبلورات السبينال مع شكل يشبه متعدد السطوح يتم التحكم فيه عن طريق الانتشار من عدد ثابت من النوى.

كلمات مفتاحية: الميليت، الكورديريت، محاليل غروية، طاقة التنشيط، معاملات أفرامي

Abstract

The mullite-cordeirite composites was prepared by Sol-Gel method, using magnesium nitrate powder, aluminum nitrate powder and tetraethyl orthosilicate solution as raw materials, these materials were mixed in various ratios according to stoichiometric formula of the wanted composite, in order to analyze the prepared materials we used several techniques, including Thermogravimetry and Differential Thermal Analysis (TG/DSC), also Dilatometry analysis to observe the phases transformation, and to confirm it we used X-ray diffraction analysis (DRX) which it been used to identify the formed phases of M50C50 which is mullite and cordierite, we also tracked the stages of phase transformations for M50C50 powder that has been treated by DSC at various temperatures using infrared technique (FTIR), by using vibration ranges we were able to identify the formed phase in various temperatures especially the amorphous phases, the activation energy and Avrami parameters for Al-Si spinal phase in the non-isothermal and isothermal treatment were calculated based on DSC analysis results, we found that the energy as the following: 605.86 kj/mol and 595.64 kj/mol respectively, as for the morphological growth parameters n and m are approximately 1.5 which indicating that the dominant crystallization volume mode in spinal phase formation followed by three dimensional growth of spinal crystals with a polyhedral-like shape controlled by diffusion from fixed number of nuclei.

Keywords : Mullite, Cordierite, Sol-Gel, Activation Energy, Avrami parameters.